

**ARI: GLOBAL REFRIGERANT ENVIRONMENTAL
EVALUATION NETWORK (GREEN) PROGRAM**

**COMPARISON OF HYDROCARBON R-290 AND
TWO HFC BLENDS R-404A AND R-410A
FOR MEDIUM TEMPERATURE REFRIGERATION
APPLICATIONS**

Final Interim Report

Date Published-March 2004

**Yunho Hwang
Dae-Hyun Jin
Reinhard Radermacher**

**CEEE
Department of Mechanical Engineering
University of Maryland**



ABSTRACT

The environmental impact of refrigerants over the entire life cycle of fluid and equipment, including power consumption, is captured in the life cycle climate performance (LCCP) value. The lower the value, the lower the environmental impact.

In this report the LCCP of hydrocarbon R-290 (Propane) and the two HFC blends, R-410A and R-404A, were evaluated for an 11 kW medium temperature refrigeration system having -18 °C to 0 °C evaporator saturated refrigerant temperature. Major findings of the current study are:

- The LCCP of R-410A is equal to that of R-290 and the LCCP of R-404A is 6.5% higher than that of R-290 for systems with condensing temperatures of 46.0°C to 47.6°C, which are representative of typical design practice.
- On an equal first cost basis, the LCCP of R-410A is 4.2% lower and the LCCP of R-404A is 1.8% higher than that of R-290. The underlying assumption is that the first cost of the R-290 system may be, for example, 10% higher due to added safety features, and on an equal cost basis, the HFC systems would use the additional cost for a larger condenser.
- Since the underlying baseline test is based on a relatively small condenser, and since a conservative safety cost estimate is used, it is expected that the environmental impact of both R-404A and R-410A would be reduced further as compared to R-290 in future system designs.

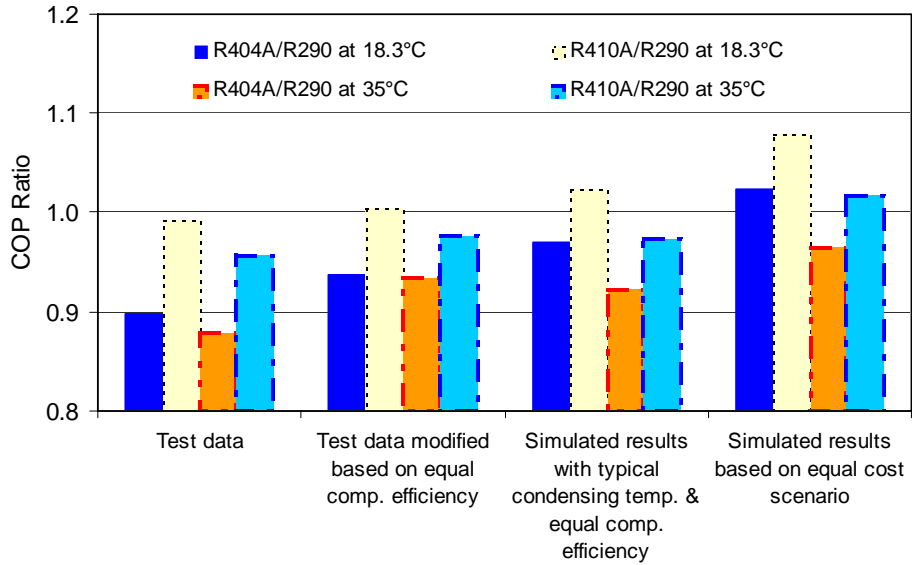
EXECUTIVE SUMMARY

Due to growing environmental awareness and resulting concerns, refrigerants, the working fluids for refrigeration systems, heat pumps and air conditioners, have attracted considerable attention. Following policies to reduce global warming, industry is developing technologies that can reduce emissions and improve energy efficiency. Despite their flammability, some refrigerator manufacturers especially in European countries and Japan have started employing hydrocarbons as refrigerants predominantly in small capacity equipment. Environmental safety issues have led to calls for the careful investigation of currently used refrigerants (HFC's) and potentially applicable HC refrigerants (R-290). To help provide a clearer understanding of the relative performance potential of the R-290 as compared to two HFC's (R-404A and R-410A) for medium temperature commercial refrigeration, CEEE started an experimental evaluation program under ARI's GREEN Program.

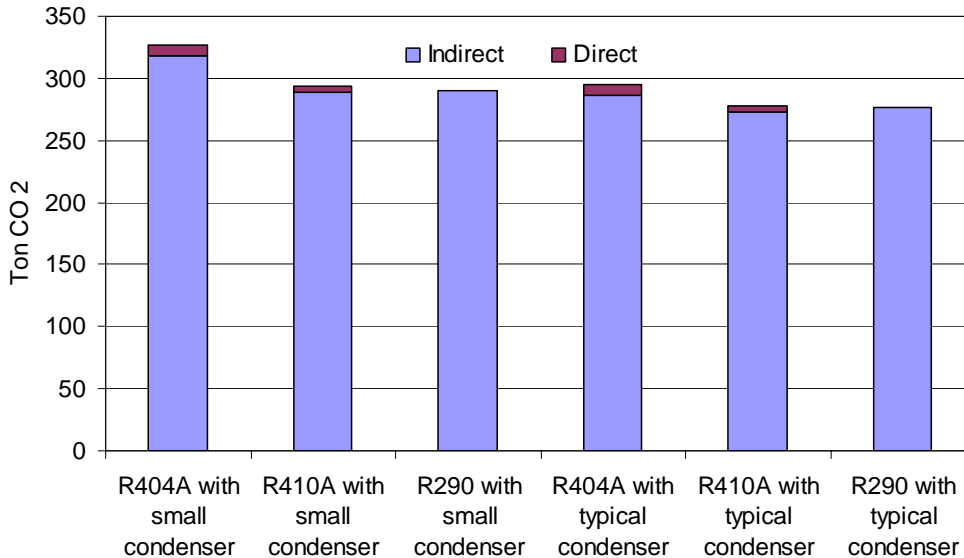
A new experimental facility to test the performance of three refrigerants for medium temperature commercial refrigeration was designed and fabricated for this study. A 11 kW refrigeration system consisting of a unit cooler and a condensing unit, which was originally designed for R-404A, served as the test unit. To match the capacity between refrigerants, compressors having a 30% smaller and 7% larger displacement volume than for R-404A were selected for R-410A and R-290. Since the displacement volume of the R-290 compressor was slightly smaller than the target displacement, a higher frequency of 66 Hz was used to match the refrigeration capacity by using an inverter drive. For safety reasons it was decided to minimize the charge of the R-290 test unit by eliminating the refrigerant receiver. The condenser was also modified to contain a liquid sub cooler circuit. In order to maintain a consistent comparison, the receiver was also eliminated from the test units for R-410A and R-404A and sub cooler circuits were added. They were designed by simulation. Based on the optimization of the condenser, which is the most critical component of the medium temperature commercial refrigeration system, a two circuit condenser was used for the testing of R-410A while a three circuit condenser was used for the testing of R-404A and R-290. The air side of all condensers was identical. By operating these systems in the newly constructed test facility, full load and part load tests were conducted under only sensible heat transfer conditions.

Once the refrigerant charge was optimized to achieve an equal system capacity under full load conditions, each refrigerant was tested both under full load and part load conditions. Then the performance comparison of the three refrigerants was extended to include three scenarios on an equal compressor efficiency basis as illustrated in Figure 14. The first scenario implies that the test data are reevaluated on an equal compressor efficiency based on the measured R-404A compressor efficiency value. The second scenario implies that a typical condenser is used for all three refrigerants. The third scenario implies that the unit first cost is matched for all three refrigerants by assuming that a typical condenser is used for only the HFC blends and additional safety features are used only for R-290. The underlying assumption is that the first cost of the R-290 system may be, for example, 10% higher due to added safety features, and on an equal cost basis, the HFC systems would use the additional cost for a larger condenser.

In order to determine the environmental impact of the refrigerants investigated, an LCCP analysis was conducted for both systems with the condenser as tested (referred to as "small condenser") and with a 48% larger condenser (referred to as "typical condenser") as illustrated in Figure 15.



Comparison of COP (Figure 14 in Report)



Comparison of LCCP (Figure 15 in Report)

Working fluid selection should consider many aspects including safety (toxicity and flammability), environmental impact (stratospheric ozone and climate change), cost and performance (capacity and COP). The two most representative commercial refrigeration configurations are the direct expansion and distributed systems, either of which could potentially release the refrigerant into human occupied space. Therefore, the use of either flammable or high toxicity refrigerants is not feasible. To limit these cases, potentially hazardous refrigerants are limited to unoccupied spaces. Thus, the R-290 LCCP value in the figure above is an artificial, best-case value. In practice, condensing units with hydrocarbon refrigerants would be used in secondary loop systems. The secondary loop system may require additional cost and energy penalties due to the additional heat exchanger and pumping requirements and the use of heat transfer fluids. Therefore, a comparison of the secondary loop R-290 system to direct HFC cooling systems should be conducted.

ACKNOWLEDGEMENTS

This work was sponsored by the Air-conditioning and Refrigeration Institute under ARI's GREEN Program. The feedback and technical guidance of the project monitoring subgroup and peer reviewers, including Warren Beeton, Richard Cawley, Piotr Domanski, Kenneth Hickman, Shaobo Jia, Kazumitsu Nishioka, Hung Pham, Ira Richter, John Sheridan and Mark Spatz, is gratefully acknowledged. Furthermore, authors acknowledge material and equipment contributions from Copeland, Heatcraft and Honeywell.

TABLE OF CONTENTS

ABSTRACT.....	ii
EXECUTIVE SUMMARY	iii
ACKNOWLEDGMENTS	v
TABLE OF CONTENTS.....	vi
LIST OF TABLES.....	vii
LIST OF FIGURES	viii
NOMENCLATURE	ix
1. INTRODUCTION	1
2. PROPERTIES OF REFRIGERANTS	2
3. HEAT TRANSFER AND PRESSURE DROP	4
4. SYSTEM PERFORMANCE MODELING.....	6
5. EXPERIMENTAL PERFORMANCE EVALUATION	8
5.1 Test Facility	8
5.2 Instrumentation and Measurement.....	9
5.3 Performance Evaluation.....	11
5.4 Error Analysis.....	13
5.5 Test Unit.....	14
5.6 Test Procedure	16
5.7 Full Load Test Results	17
5.8 Part Load Test Results	23
5.9 Comparison of Simulation and Experimental Results	23
6. LIFE CYCLE CLIMATE PERFORMANCE (LCCP) ANALYSIS	25
6.1 Safety Issue and Energy Efficiency	25
6.2 LCCP Comparison.....	27
7. CONCLUSIONS.....	28
8. REFERENCES	30

LIST OF TABLES

Table 1: Environmental Effects of Some Refrigerants (UNEP, 2002))	1
Table 2: Thermophysical Properties of Three Refrigerants (NIST, 2002).....	3
Table 3: Simulated COP of the Investigated Condenser Circuits.....	7
Table 4: Measurement Errors.....	13
Table 5: Specifications of Heat Exchangers	15
Table 6: Specifications of Compressors	15
Table 7: Impurities of Propane (Airgas, 2003)	16
Table 8: Test Conditions.....	17
Table 9: Effects of Using Inverter on Electrical Characteristics and Performance of R-410A.....	17
Table 10: Full Load Test Results (Optimum charge in bold).....	20
Table 11: Thermodynamic Comparison of Three Refrigerants.....	21
Table 12: Contribution of Condensation Heat Transfer	21
Table 13: Effects of Compressor Efficiency under Full Load Conditions	22
Table 14: Part Load Test Results	23
Table 15: Effects of Compressor Efficiency under Part Load Conditions	24
Table 16: Comparison of Cycle Parameters between Model and Test Results	25
Table 17: Effects of Condenser on Condensing Temperature	25
Table 18: Effects of Condenser on Compressor Efficiency under Full Load Conditions	26
Table 19: System Power Consumption - Weather Bin Analysis	27

LIST OF FIGURES

Figure 1: Saturation Pressure of Refrigerants.....	2
Figure 2: Comparison of Thermophysical Properties.....	3
Figure 3: Comparison of Theoretical Cycle Efficiency.....	4
Figure 4: Heat Transfer Characteristics of Refrigerants.....	5
Figure 5: Pressure Drop Characteristics of Refrigerants.....	5
Figure 6: Effects of Conductance on HX Effectiveness of the Evaporator.....	6
Figure 7: Condenser Circuits.....	7
Figure 8: Test Facility for Unit Cooler.....	8
Figure 9: Test Facility for Condensing Unit.....	9
Figure 10: Heat Exchanger Circuits and Instrumentation.....	14
Figure 11: Charge Optimization Results.....	18
Figure 12: Compressor Efficiency vs. Pressure Ratio.....	22
Figure 13: Comparison of Simulation and Experimental Results.....	24
Figure 14: Comparison of COP.....	26
Figure 15: Comparison of LCCP.....	28

NOMENCLATURE

A	Throat area of the orifice
CEEE	Center for Environmental Energy Engineering
CFC's	Chlorofluorocarbons
COP	Coefficient Of Performance
Cp_a	Specific heat of air
DP_{cond}	Pressure drop across the condenser
DP_{evap}	Pressure drop across the evaporator
EES	Engineering Equation Solver
F	Function
GREEN	Global Refrigerant Environmental Evaluation Network
GWP	Global Warming Potential
h_{in}	Enthalpy of refrigerant at the indoor unit inlet
h_{out}	Enthalpy of refrigerant at the indoor unit outlet
$h_a A_a$	Air-side conductance
$h_{dis,isen}$	Enthalpy of refrigerant when the suction gas is isentropically compressed
h_{suc}	Enthalpy of refrigerant at the compressor suction
$h_r A_r$	Refrigerant-side conductance
HC's	Hydrocarbons
HCFC's	Hydrochlorofluorocarbons
HFC's	Hydrofluorocarbons
HX	Heat exchanger
LCCP	Life Cycle Climate Performance
\dot{m}_r	Refrigerant mass flow rate
n	Number of variables
$P_{cond,avg}$	Average pressure of inlet and outlet of the condenser in absolute pressure
$P_{evap,avg}$	Average pressure of inlet and outlet of the evaporator in absolute pressure
PR	Ratio between the discharge and suction pressure
V	Volumetric air flow rate
Q_{air}	Air-side capacity
Q_{ref}	Refrigerant-side capacity
q_{lci}	Latent air-side capacity
q_{sci}	Sensible air-side capacity
RPM	Revolution Per Minute
T_{ain}	Air temperature entering the indoor unit
T_{aout}	Air temperature leaving the indoor unit
T_{cond}	Condensing temperature
T_{evap}	Evaporating temperature
T_{suc}	Refrigerant temperature at the compressor suction
TEWI	Total Equivalent Warming Impact
TXV	Thermal expansion valve
u_F	Uncertainty of the function
u_n	Uncertainty of the parameter
V_{disp}	Compressor displacement volume
v_n	Parameter of interest (measurement)

v'_n	Specific volume of air at orifice throat
W_n	Humidity ratio of air at orifice throat
W_{in}	Humidity ratio of air entering the indoor unit
W_{iout}	Humidity ratio of air leaving the indoor unit
W_{comp}	Power consumption of the compressor
W_{total}	Power consumption of the compressor, fans of the unit cooler and condensing unit
ρ	Density of the air
ρ_{suc}	Density of refrigerant at the compressor suction
ΔP	Pressure drop across the orifice
η_{vol}	Volumetric efficiency
η_{comp}	Compressor efficiency

1 INTRODUCTION

Refrigerants should satisfy thermodynamic requirements to efficiently deliver sufficient capacities while being locally and globally safe. Among the three natural refrigerants listed in Table 1, hydrocarbons (HC's) such as propane (R-290), isobutane (R-600a), cyclopropane (RC-270), and their mixtures are already being used especially in some part of the European Union (EU) and Japan, predominantly in domestic refrigerators due to their environmentally benign characteristics. In 1992, DKK Scharfenstein in Germany developed refrigerators using HC's for both the blowing of insulation foam and the refrigerant (Greenpeace, 1997). Since then, the major household appliance manufacturers in the EU have been marketing HC's based refrigerators. In Japan most of major refrigerator companies have introduced HC's based refrigerators in 2002 (JARN, 2002). The charge of HC's in the refrigerator is very small, about 20 grams in a 130 liter refrigerator, which is almost equivalent to the charge in a cigarette lighter. The use of HC's is growing but their flammability restricts them in other applications where a large quantity of refrigerant is needed such as commercial refrigeration applications. Commercial refrigeration applications include self-contained refrigeration systems similar to domestic refrigerators but also large scale and central refrigeration systems connected to remote evaporators.

Table 1: Environmental Effects of Some Refrigerants (UNEP, 2002)

Refrigerants		ODP	GWP (Time horizons of 100 yrs)
HCFC's	R-22	0.055	1,700
HFC's	R-134a	0	1,300
	R-404A (R125/143a/134a)	0	3,800
	R-410A (R32/125)	0	2,000
Natural Refrigerants	Carbon dioxide (R-744)	0	1
	Ammonia (R-717)	0	<1
	Propane (R-290)	0	20
	Isobutane (R-600a)	0	20
	Cyclopropane (RC-270)	0	n/a

GREEN Program

The International Council of Air-Conditioning and Refrigeration Manufacturers' Associations (ICARMA) established in 1991 initiated the Global Refrigerant Environmental Evaluation Network (GREEN) Program in 2001. In 2003, under the GREEN Program, the Center for Environmental Energy Engineering (CEEE) of the University of Maryland jointly with Copeland, Heatcraft, Honeywell, and ARI started a testing program to develop technically unbiased, credible refrigerant performance information on new and existing refrigerants in a variety of refrigeration, air conditioning, and heat pump applications. The objective of the program is to conclusively establish the relative performance potential of HFC's (R-404A, and R-410A) as compared to R-290 using a 11 kW capacity system for medium temperature commercial refrigeration having -18°C to 0°C evaporator saturated refrigerant temperature, which is designed without the receiver and is critically charged. The choice to operate the refrigeration systems without a receiver was made in order to minimize the refrigerant charge in the test rig for safety reasons as well as for the experiments to verify modeling results that also did not include a receiver.

2 PROPERTIES OF REFRIGERANTS

Figure 1 shows the saturation pressures of three refrigerants of interest. While R-410A has 33% consistently higher vapor pressure than that of R-404A, the saturation pressure of R-290 is 14% lower at -50°C and 27% lower at 70°C , which indicates a smaller pressure ratio at the same operating temperature levels.

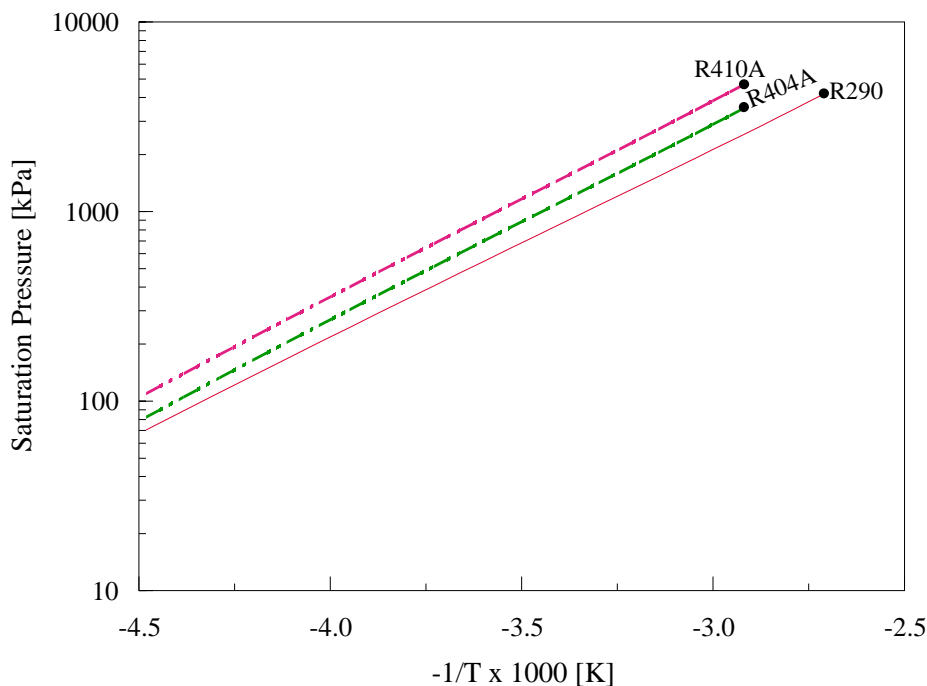
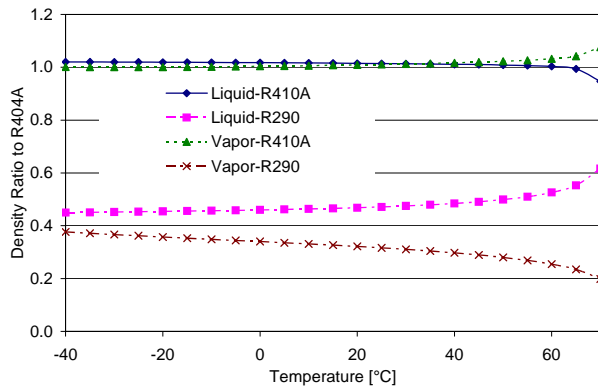


Figure 1: Saturation Pressure of Refrigerants

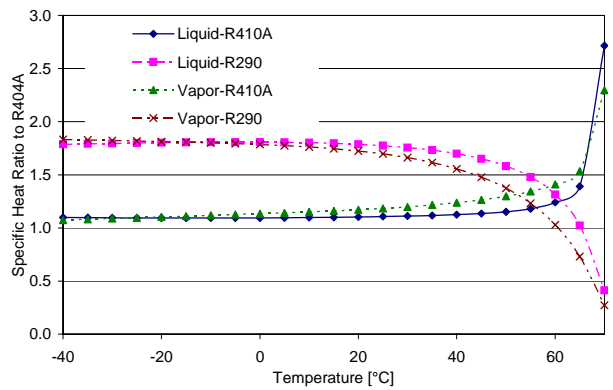
The thermophysical properties of the three refrigerants are compared at typical evaporating and condensing temperatures for medium temperature refrigeration applications as shown in Table 2. Both R-410A and R-290 show higher liquid- and vapor-specific heat and liquid thermal conductivity than those of R-404A. While R-410A has a 5% lower liquid viscosity and similar vapor viscosity as R-404A, R-290 has a 17 to 30% lower liquid viscosity and about 40% lower vapor viscosity. Figure 2 shows the relative values of these properties of R-410A and R-290 as compared to those of R-404A over the temperature range between -40°C and 70°C . Overall, it is expected that R-290 would have the best transport properties among the three refrigerants and R-410A would have better transport properties than R-404A. While the volumetric capacity of R-410A is 34% higher than that of R-404A, the volumetric capacity of R-290 is 23% lower than that of R-404A, which means a smaller and bigger compressor displacement volume is required for R-410A and R-290, respectively. It should be noted that thermophysical properties change significantly when the temperature exceeds approximately 60°C as can be seen from Figures 2 and 3. This is because R-404A and R-410A are approaching the critical point where thermophysical properties change significantly while R-290 does not.

Table 2: Thermophysical Properties of Three Refrigerants (NIST, 2002)

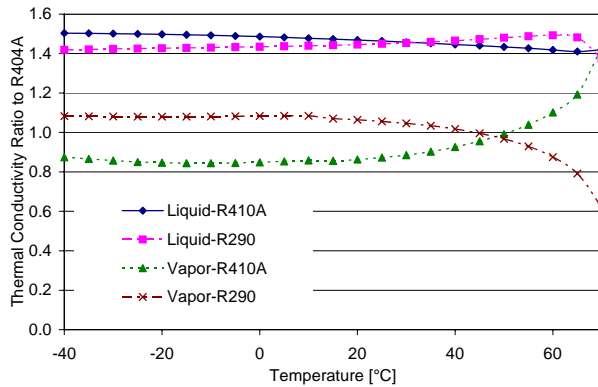
Refrigerant	R-404A		R-410A		R-290	
	-5°C	50°C	-5°C	50°C	-5°C	50°C
Molecular mass [g/mol]	97.6		72.6		44.1	
Normal boiling point [°C]	-46.1		-51.7		-42.1	
Critical temperature [°C]	72.0		71.4		96.7	
Critical pressure [MPa]	3.7		4.9		4.2	
Saturation pressure [kPa]	515	2,304	679	3,067	406	1,713
Sat. liquid density [kg/m ³]	1,169	899	1,190	907	535	449
Sat. vapor density [kg/m ³]	25.9	138	26.0	141	8.9	38.7
Sat. liquid specific heat [kJ/kg-K]	1.37	1.96	1.50	2.26	2.47	3.10
Sat. vapor specific heat [kJ/kg-K]	0.97	1.85	1.09	2.40	1.74	2.54
Sat. liquid viscosity [μ Pa-s]	191	89	182	84	132	74
Sat. vapor viscosity [μ Pa-s]	12.3	17.3	12.3	17.4	7.3	9.4
Sat. liquid thermal conductivity [mW/m-K]	75.9	55.7	113	79.9	109	82
Sat. vapor thermal conductivity [mW/m-K]	14.0	24.3	11.9	24.1	15.2	23.5
Latent heat [kJ/kg]	170	104	227	136	382	284
Volumetric capacity [kJ/ m ³]	4,406	-	5,900	-	3,396	-



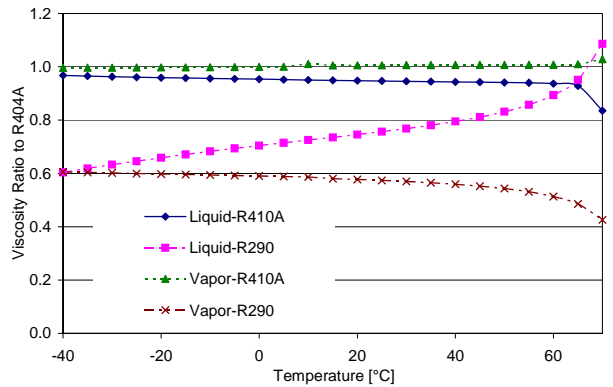
(a) Density



(b) Specific heat



(c) Thermal conductivity



(d) Viscosity

Figure 2: Comparison of Thermophysical Properties

Figure 3 illustrates the comparison of the theoretical cycle efficiency of the three refrigerants for various condensing temperatures but a fixed evaporating temperature of the -6.7°C when ideal cycle conditions are used (zero subcooling, zero superheating, zero pressure drop across the heat exchangers, 100% compressor efficiency). This comparison shows that the three refrigerants have similar performance at low condensing temperatures (within 2% at 15.6°C condensing temperature) but R-410A and R-290 perform better than R-404A at higher condensing temperatures (10% and 17% better, respectively at 50°C condensing temperature).

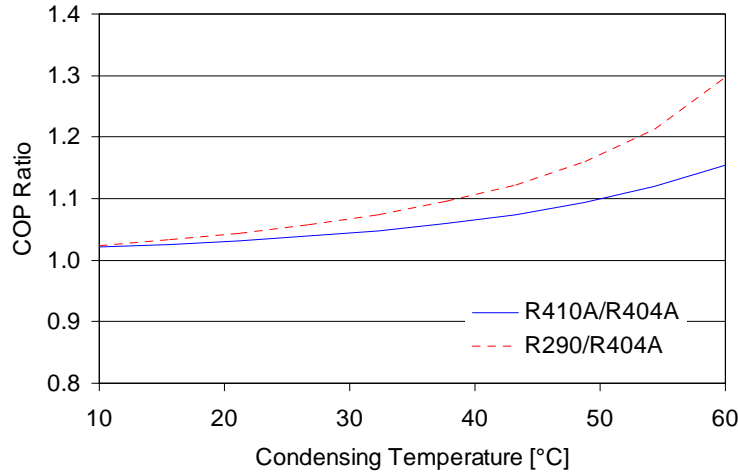
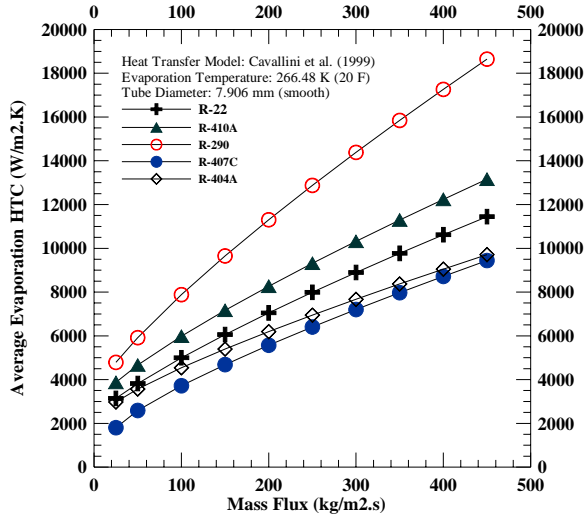


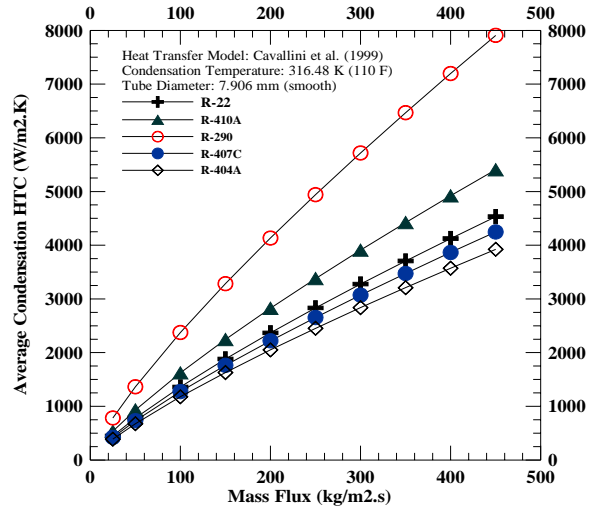
Figure 3: Comparison of Theoretical Cycle Efficiency

3 HEAT TRANSFER AND PRESSURE DROP

For better comparison of the effect of transport properties, information on the heat transfer and pressure drop characteristics of these refrigerants are required. Figures 4 and 5 show predictions of average heat transfer coefficients and pressure drop for all refrigerants used in this study (Spatz and Motta, 2003). To verify that these predictions are in agreement with previous publications (Chin and Spatz, 1999; Bivens et al., 1993) predictions on R-22 and R-407C are included as well. At the same mass flux, R-290 has the best heat transfer among all these refrigerants, but it also suffers the highest pressure drop penalty. These results were expected since the vapor density of R-290 is the lowest, and this property has a large impact in pressure drop predictions. R-410A has superior heat transfer than R-22 and R-404A. Pressure drop plots also show that R-410A suffers the lowest penalty among all the alternatives, which allows further optimization of the heat exchangers design. However, actual comparisons must be conducted at the actual mass fluxes in the system circuits since their mass flow fluxes are different when the system is designed for each refrigerant to produce the same capacity.

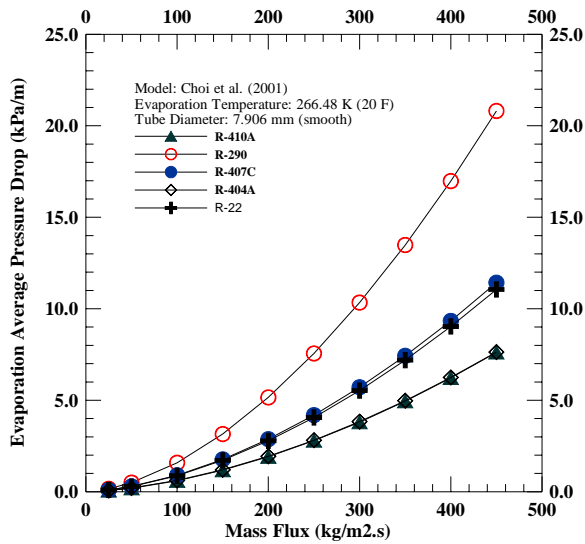


(a) Evaporation Heat Transfer

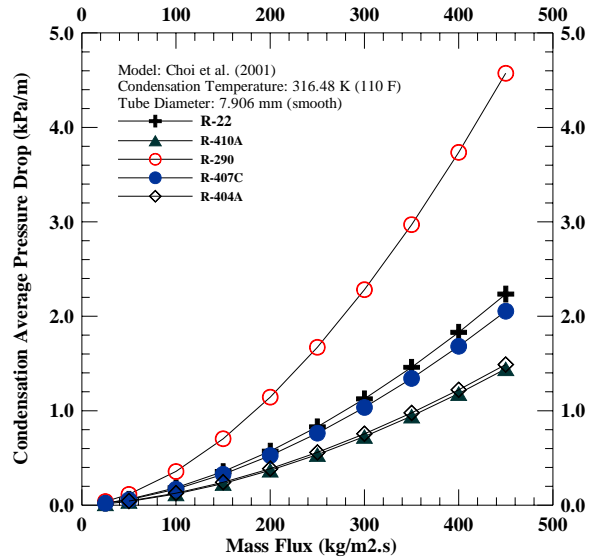


(b) Condensation Heat Transfer

Figure 4: Heat Transfer Characteristics of Refrigerants



(a) Evaporation Pressure Drop



(b) Condensation Pressure Drop

Figure 5: Pressure Drop Characteristics of Refrigerants

4 SYSTEM PERFORMANCE MODELING

In order to evaluate the system with different refrigerants and make changes to the coil circuit that better suits a particular refrigerant, a detailed system model was used. The model employed for the simulations, Honeywell's Genesym™, represents a vapor compression refrigeration cycle operating at steady-state conditions. The overall model is composed of sub-models for each component of the system. The major component models include:

- Compressor: Map based and analytical models;
- Evaporator and Condenser: Detailed tube-by-tube modeling;
- Expansion Devices: Analytical models (capillary tubes) and empirical correlations (short tubes, expansion valves).

For an independent verification of the modeling effort, the test and modeling results were also reproduced with "Coil Designer" and "Vapcyc" of CEEE, which are simulation tools for heat exchangers and vapor compression refrigeration cycles.

To model each component, the energy, momentum and mass balance equations are applied together with heat transfer laws, when necessary. This model incorporates some of the most relevant features of existing models, including quasi-local heat transfer analysis of heat exchangers (Domanski, 1989) and simulation of thermostatic expansion devices. Properties are calculated using REFPROP 7 (NIST, 2002), therefore any pure fluid or mixture present in this database can be used in the model. The models for air-side heat transfer coefficient employed were developed by Wang et al. (2000, 1999a, 2001, 1999b) for flat, wavy, lanced, and louvered fins, respectively. Condensation and evaporation refrigerant-side heat transfer coefficients were developed by Cavallini et al. (1999). The two-phase pressure drop models are from Choi et al. (1999).

When running the model to simulate and optimize the performance of the test system for a particular refrigerant, it was observed that due to the low air-side fin density that is typical of this type of commercial refrigeration equipment, there was little performance impact of circuit changes (especially in the evaporator). Figure 6 graphically shows the relationship between refrigerant-side conductance ($h_r A_r$), air-side conductance ($h_a A_a$), and the overall impact on heat exchanger effectiveness of the evaporator when either refrigerant-side conductance or air-side conductance is fixed while the other conductance is varied.

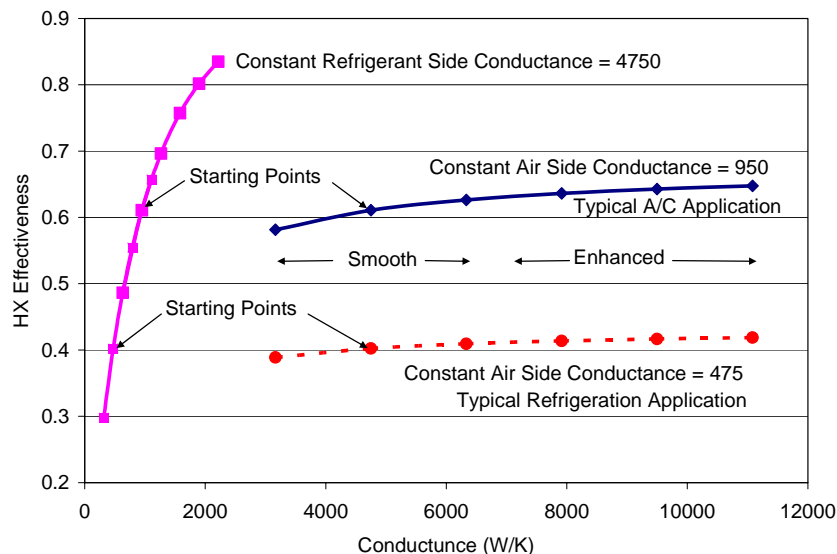


Figure 6: Effects of Conductance on HX Effectiveness of the Evaporator

The low air-side conductance values in the lower portion of the graph represent typical values for commercial refrigeration systems. Re-circuiting the refrigerant path circuits to obtain higher heat transfer coefficients and thereby increasing the refrigerant-side conductance, does not significantly increase the heat exchanger effectiveness. There is more opportunity for improvement in air-conditioning applications where the higher fin density increases the air-side conductance values.

Simulation results showed no significant change in system efficiency when the number of circuits was changed for any of the refrigerants since this heat exchanger has only 3.6 mm fin pitch on the airside. With a slightly higher fin density for the condenser (2.1 mm fin pitch), there was somewhat more opportunity for optimizing circuit for this component. Figure 7 shows five condenser circuits investigated in this study. The results of this optimization are shown in Table 3. There is not a significant impact of the circuitry changes on system efficiency (around 1% or less). The results shown are for the optimum subcooling found from the charge optimization test. For each refrigerant, the circuit corresponding to the COP value in bold was the one used for testing. It should be noted that the 2:1 circuit with 18 tube subcooling circuit was chosen for R-410A testing because it resulted in the highest COP or close to the highest COP when the degree of subcooling is either at the optimum or lower than the optimum.

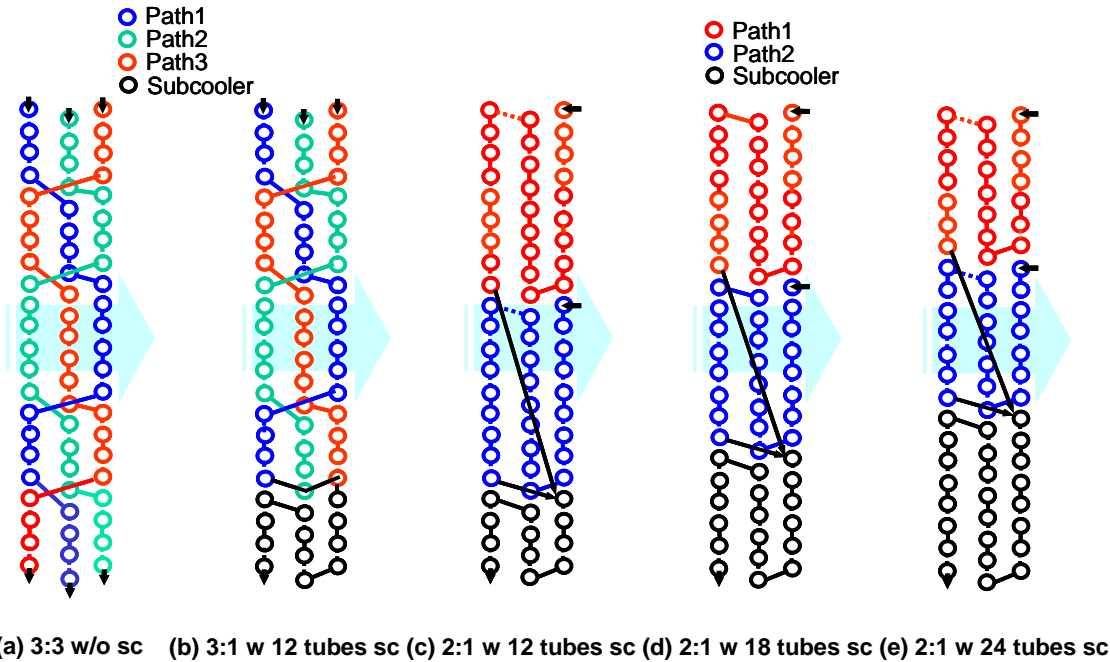


Figure 7: Condenser Circuits

Table 3: Simulated COP of the Investigated Condenser Circuits

Circuit	COP		
	R-404A	R-410A	R-290
3:3 circuits without subcooling circuit	1.61	n/a	n/a
3:1 circuit with 12 tube subcooling circuit	1.61	1.75	1.87
2:1 circuit with 12 tube subcooling circuit	1.59	1.76	1.84
2:1 circuit with 18 tube subcooling circuit	1.58	1.75	1.86
2:1 circuit with 24 tube subcooling circuit	n/a	1.75	n/a

5 EXPERIMENTAL PERFORMANCE EVALUATION

Since the reduction of global warming is a major focus for the comparison of refrigerants, the coefficient of performance (COP) of each refrigerant is of concern. However, the performance of HFC's as well as HC's varies much depending upon the test conditions and the degree of system modifications. To contribute to a clearer understanding of the relative performance potential of each refrigerant, the hardware was optimized for each refrigerant in the current study.

5.1 Test Facility

The performance of the test unit was measured through the use of a psychrometric test facility constructed at CEEE's heat pump laboratory. This system is comprised of an air duct and two environmental chambers, which housed the indoor and outdoor heat exchangers and the compressor, to measure the capacity based on ARI Standard 420 for unit coolers for refrigeration (ARI, 2000) and ARI Standard 520 for positive displacement condensing units (ARI, 1997). The arrangement of the test facility is shown in Figures 8 and 9. The unit cooler and the condensing unit were separated from each other through the use of two environmental chambers capable of achieving temperatures ranging from -6 to 43°C, allowing for the independent control of the inlet air stream conditions. As shown in Figure 8, the indoor duct is equipped with dew point meters to measure the dry bulb and dew temperatures of the air, and an orifice plate to measure the air flow rate. The desired air flow rate was adjusted by an inverter that controlled the speed of a fan which was installed in addition to the original evaporator fans and located in the outlet of the air duct to overcome the additional pressure drop caused by mixing devices, orifice plate, and duct. The duct outlet is open to the chamber to recondition the air stream, after which the air returns to the test unit. This air duct is sealed by a duct sealant, to prevent air leakage, and wrapped with insulation to prevent heat losses.

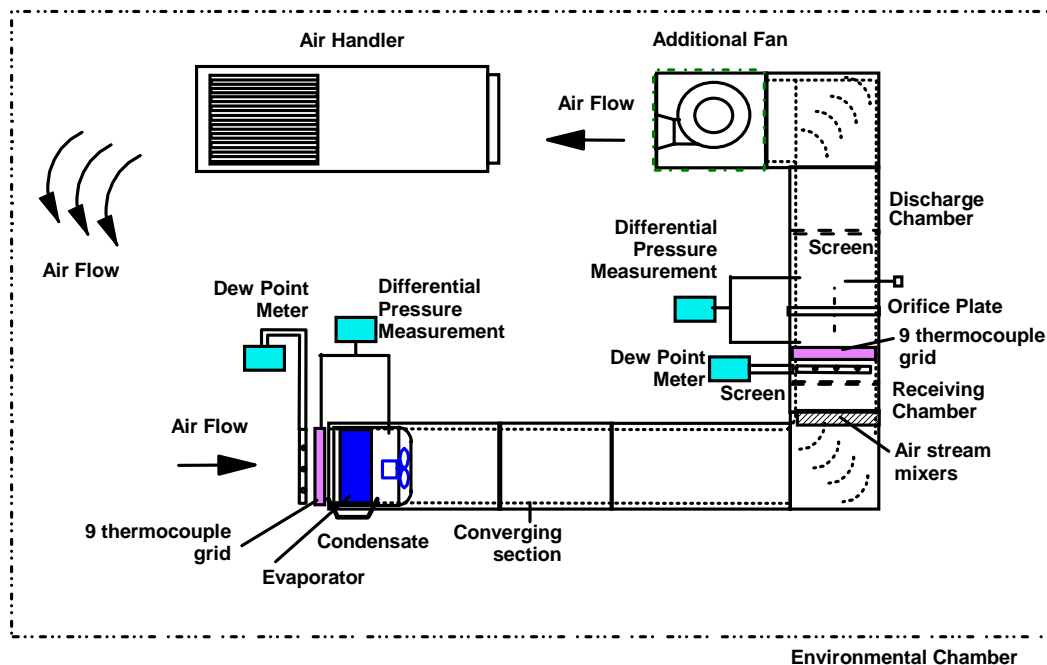


Figure 8: Test Facility for Unit Cooler

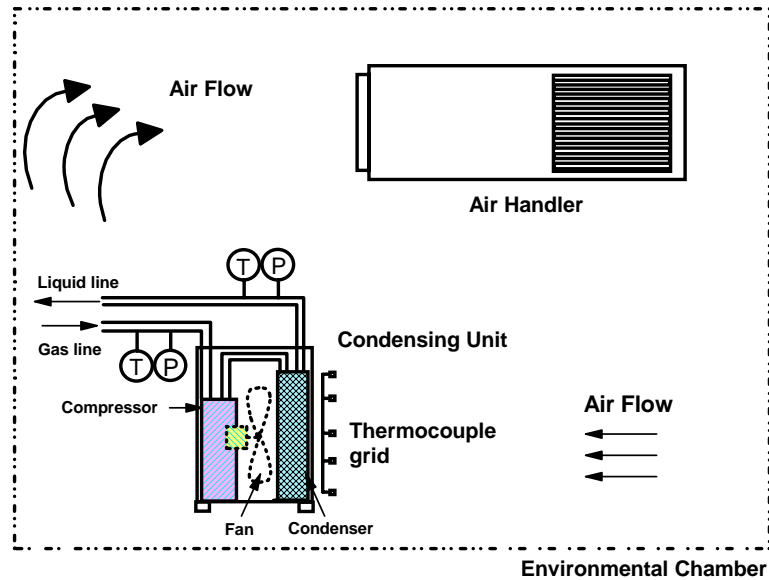


Figure 9: Test Facility for Condensing Unit

The duct size was determined according to ASHRAE Standard 40 (1980), which suggests the duct section be sized for velocities of 5.6-6.6 m/s. From the air flow rate, $3.3 \text{ m}^3/\text{s}$, appropriate for the given test unit, the duct size was determined to be 66 cm by 76 cm. A tube-axial fan, which has a 56 cm propeller diameter supplies up to 570 Pa at $3.3 \text{ m}^3/\text{s}$.

5.2 Instrumentation and Measurement

Along with the test facility, instrumentation to measure the performance of the test unit was implemented. The instrumentation was designed to determine the properties of air and refrigerant. There are basically four types of measurements necessary to obtain the required data to calculate and evaluate the performance of the test unit. These are temperatures, pressures, mass flow rate, and power.

Temperature Measurement

To measure the temperature of the air and the refrigerant, T type copper-constantan thermocouples with an accuracy of $\pm 0.2 \text{ }^\circ\text{C}$ were employed. To measure the inlet and outlet air stream temperature of an evaporator, two thermocouple grids, which have nine thermocouples each, were installed at the inlet and outlet of the unit cooler after the air mixer. Temperature difference between these two thermocouple grids was calibrated such that it is zero when there is no heat transfer in the duct section between the thermocouple grids. For the outdoor unit, nine thermocouples were installed at both the air inlet and outlet. To measure the bulk temperature of the refrigerant, in-stream thermocouples were installed at all inlets and outlets of all components.

The upstream and downstream air side dew points in the test duct were measured using chilled mirror devices with an accuracy of $\pm 0.2 \text{ }^\circ\text{C}$ of the coupon temperature. These units were routinely cleaned and calibrated against internal settings to insure proper operation.

Pressure Measurement

For the pressure measurement of the air and refrigerant, piezoelectric pressure transducers were installed. The static pressures for the air duct were measured with differential pressure transducers with a range of 0 to 650 Pa and an accuracy of $\pm 1\%$ full scale. Absolute

pressure transducers having accuracies of 0.11% full scale were used to measure the refrigerant pressures. These absolute measurements were also made in conjunction with differential pressure transducers used to more accurately measure the pressure drop across the evaporator. The transducers were directly connected to the piping system with tees. The transducers were calibrated by utilizing a pressure calibrator (Omega, PCL5000) after installation into the system. The correlation obtained from the calibration was used in the data acquisition program to convert voltage output into pressure values.

Refrigerant Mass Flow Rate Measurement

Refrigerant mass flow was measured with a Coriolis type mass flow meter with an accuracy of $\pm 0.4\%$, which was placed downstream of the condenser outlet. The output signal of 4-20 mA was adjusted to correspond to a range of 0-300 g/s for R-404A, 0-100 g/s for R-410A and R-290 by using a transmitter calibrator.

Air Volume Flow Rate Measurement

As shown in Figure 8, differential pressure transducers were used for measurement of the air side pressure drop across the flow measurement device. This pressure differential measurement across the flow measurement device was used to determine the volumetric air flow rate (V) in the duct by equation (1) (ASHRAE Handbook, 2001).

$$V = K * A * \sqrt{\frac{2 * \Delta P}{\rho}} \quad (1)$$

where K is a constant determined by combining C , a friction loss coefficient factor, with $1/(1-\beta^4)^{0.5}$ which is an approach factor. The coefficient A refers to the area of the orifice, ρ is the density of the air, and ΔP is a pressure drop across the orifice.

The size of the orifice was determined to be 51 cm to keep the pressure drop close to 360 Pa. A constant K was calibrated by using a bank of finned strip heaters having a 9 kW capacity, which were placed between the unit cooler and the orifice.

Compressor RPM Measurement

A piezoelectric accelerometer was used to measure compressor speed.

Power Measurement

The input power to the unit cooler fans and the outdoor fan was measured with watt transducers having an accuracy of $\pm 0.2\%$ full scale. For the R-404A compressor, the compressor power was measured with a power transducer with a range of 0-40 kW and an accuracy of $\pm 0.2\%$ full scale for a three phase 60 Hz signal. Since an inverter was used to exactly match the cooling capacity of R-290 and R-410A to that of R-404A, input power and line voltage of the R-290 and R-410A compressors were measured before and after the inverter with a digital power meter (Yokogawa, WT-1600) having an accuracy of 0.3%.

Measurement of Refrigerant Charges and Water Condensate

An electronic scale having an accuracy of 1 g is used for charging the refrigerant. The electronic scale having an accuracy of 0.1 g is used for weighing the water condensate.

Data Acquisition

Signals from all instruments were fed to a LabView data acquisition software package through the use of National Instruments' FieldPoint DAQ modules. These modules allow for flexibility in instrumentation, as additional channels may be added or removed easily if required later. These modules may also be placed close to the individual parts of the experiment (rather than the computer), eliminating both excessive cable lengths, and problems arising from incorrect wiring. A total of 96 channels of data were collected (64 thermocouples and 32 analog inputs) and sent to the computer for collection and instantaneous on-screen visualization of system parameters (e.g. pressures, temperatures, air flow rates, etc.). The tested sampling rate of this system was 5 seconds. A GUI was written for this experiment, allowing the user quick access to data from the system as it was in operation. Numeric outputs monitored include air side temperatures, air flow rates, dew points, performance (including COP, compressor work, and both latent and sensible cooling loads), refrigerant pressures, mass flow rate, and in-stream temperatures. The graphical portion of the program monitored the history of many of these same measurements. When all measured data reached steady state within 1% variation (temperature variation less than 0.1°C) for more than 30 minutes, the data collection was started for 30 minutes at 5 seconds interval.

5.3 Performance Evaluation

The performance of the test unit was evaluated in terms of its capacity, COP, and compressor efficiencies as described below. To evaluate the capacity experimentally, the air-side capacity and refrigerant-side capacity were calculated from the measured data.

Air-Side Capacity

The sensible air-side capacity (q_{si}) was calculated by equation (2) (ASHRAE Standard 37, 1988).

$$q_{si} = \frac{V}{v'_n(1+W_n)} Cp_a (T_{ain} - T_{aout}) \quad (2)$$

where Cp_a : Specific heat of air
 T_{ain} : Air temperature entering the indoor unit
 T_{aout} : Air temperature leaving the indoor unit
 v'_n : Specific volume of air at orifice throat
 W_n : Humidity ratio of air at orifice throat

The latent air-side capacity (q_{lci}) was calculated from the humidity ratio difference between inlet and outlet by equation (3).

$$q_{lci} = 2.47 \times 10^6 \frac{Q}{v'_n(1+W_n)} (W_{iin} - W_{iout}) \quad (3)$$

where W_{iin} : Humidity ratio of air entering the indoor unit
 W_{iout} : Humidity ratio of air leaving the indoor unit

Then the air-side capacity (Q_{air}) was calculated by summing up the sensible air-side capacity (q_{sci}) and the latent air-side capacity (q_{lci}). It should be noted that the latent air-side capacity was zero for all cases in this study by maintaining the dew temperature of the chamber air lower than

the evaporator surface temperature. This was confirmed by observing the coil condition and checking for condensate after each test.

Refrigerant-Side Capacity

The refrigerant-side capacity (Q_{ref}) was calculated using the mass flow rate of refrigerant and enthalpy difference between inlet and outlet of the evaporator. The evaporator inlet enthalpy was obtained from the expansion valve inlet enthalpy by assuming an isenthalpic expansion process. These enthalpies were calculated based on the measured pressures and temperatures by using thermodynamic property routines, REFPROP V7 (NIST, 2002). Then the refrigerant-side capacity (Q_{ref}) was calculated using equations (4).

$$Q_{ref} = \dot{m}_r (h_{out} - h_{in}) \quad (4)$$

where \dot{m}_r : refrigerant mass flow rate

h_{in} : enthalpy of refrigerant at the indoor unit inlet

h_{out} : enthalpy of refrigerant at the indoor unit outlet

To confirm that the data are reliable, the capacity determined using these two methods should agree within 6% of each other as required by ASHRAE Standard 116 (1995). The two methods agreed within 3% for all tests conducted in this study. The reported capacity and COP values were based on refrigerant-side values. The air-side values were used only to check the total energy balance.

COPs

COPs were calculated for both the air-side and the refrigerant-side based on the capacity and total system power consumption (W_{total}) including the condenser and unit cooler fan motor power consumption in addition to the compressor power consumption by using equation (5).

$$\begin{aligned} COP_{air} &= Q_{air} / W_{total} \\ COP_{ref} &= Q_{ref} / W_{total} \end{aligned} \quad (5)$$

Compressor Efficiencies

For the compressor performance evaluation, volumetric (η_{vol}) and compressor (η_{comp}) efficiencies were calculated as defined by equations (6) and (7) (ASHRAE, 2000; ARI, 1997):

$$\eta_{vol} = \frac{\dot{m}_r}{\rho_{suc} \times V_{disp} \times RPM / 60} \quad (6)$$

$$\eta_{comp} = \frac{(h_{dis,isen} - h_{suc}) * \dot{m}_r}{W_{comp}} \quad (7)$$

where ρ_{suc} : refrigerant density at the compressor suction

V_{disp} : compressor displacement volume

RPM : compressor revolution speed

$h_{dis,isen}$: refrigerant enthalpy when the suction gas is isentropically compressed

h_{suc} : refrigerant enthalpy at the compressor suction

W_{comp} : compressor power consumption

5.4 Error Analysis

During experimentation, bias (or systematic) error and the precision error are two important parameters to be mindful of (Beckwith et al., 1993). Detailed error analysis to determine the magnitude of these values is described as follows.

Bias Error

The total uncertainty of a measurement due to the uncertainty of individual parameters is referred to as the propagation of uncertainty (Beckwith et al., 1993). Also referred to as bias, the total uncertainty of any function may be calculated using the Pythagorean summation of uncertainties which is defined by equation (8) (Kline and McClintock, 1953):

$$u_F = \sqrt{\left(\frac{\partial F}{\partial v_1} * u_1\right)^2 + \left(\frac{\partial F}{\partial v_2} * u_2\right)^2 + \left(\frac{\partial F}{\partial v_3} * u_3\right)^2 + \dots + \left(\frac{\partial F}{\partial v_n} * u_n\right)^2} \quad (8)$$

where:

- u_F = uncertainty of the function
- u_n = uncertainty of the parameter
- F = function
- v_n = parameter of interest (measurement)
- n = number of variables

The partial derivatives of each independent measurement for the relevant calculated parameters were determined using the uncertainty propagation function in the Engineering Equation Solver (EES), and applied within the program to the root mean square (rms) outcome. The results of this effort are shown in Table 4.

Precision Error

Precision error is an uncertainty that occurs in the same way each time a measurement is made. This minimum/maximum error in the measurements of importance was calculated with a spreadsheet based upon the rated deviation of the system's instrumentation. The precision error was calculated to have a confidence level of 99.7%.

Total Error

After evaluating the bias and precision errors, the total errors are calculated by summing up these two errors. Table 4 shows the results of the total error calculation applied to those quantities important in this study. From this, it was determined that the air side calculations for capacity and COP generated the most uncertainty, primarily due to the accuracy of the instruments involved in the measurement (thermocouple grids, air side pressure transducers and dew point meters), and this is the reason for reporting the refrigerant-side performance as the primary method.

Table 4: Measurement Errors

Parameter	Air-side capacity	Air-side COP	Refrigerant-side capacity	Refrigerant-side COP
Bias error [%]	0.8	0.8	1.1	1.8
Precision error [%]	1.6	1.6	0.4	0.5
Total error [%]	2.4	2.4	1.5	2.3

5.5 Test Unit

The test unit consists of a unit cooler and a condensing unit having a 11 kW refrigeration capacity for medium temperature refrigeration having -18°C to 0°C evaporator saturated refrigerant temperature and both designed for R-404A. A unit cooler incorporates three fans that produce a flow rate of $3.3\text{ m}^3/\text{s}$ with a capacity of 11 kW at -4°C evaporator saturated refrigerant temperature. The condensing unit has a single axial fan delivering an air flow rate $1.6\text{ m}^3/\text{s}$ and has a rated a capacity of 15 kW at an ambient temperature of 35°C . The refrigeration cycle of the test unit is shown in Figure 10.

Heat Exchangers

The evaporator has 9 circuits and each circuit consists of 6 tubes in three rows. Each circuit is distributed along the vertical direction. The overall flow direction of the refrigerant is against the air stream. The receiver was omitted to minimize the refrigerant charge levels and therefore to increase safety when R-290 is used. To maintain consistency in the testing with the simulation, which assumed the system was not equipped with a receiver, the condenser circuit was redesigned to have a subcooler. Based on the simulation described earlier, the same condenser, but two different circuits, was used in testing. A three circuit condenser (Figure 10 (a)) was used for testing of R-404A and R-290, and a two circuit condenser (Figure 10 (b)) was used for testing of R-410A. The three circuit condenser consists of 18 tubes in each circuit and the three circuits join just before the last 12 tubes to form the subcooler. The two circuit condenser consists of 24 tubes in each circuit and they join just before the last 18 tubes to form the subcooler.

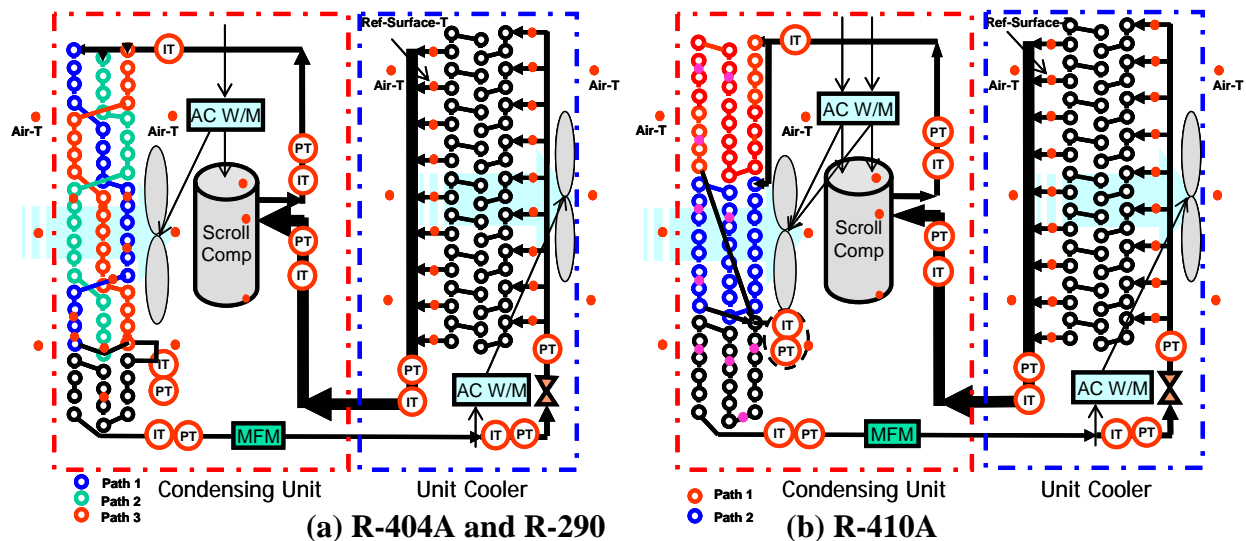


Figure 10: Heat Exchanger Circuits and Instrumentation

Details of both heat exchangers are listed in Table 5. The measured surface temperatures of the inlet and outlet of each condenser circuit for all three refrigerants were comparable within 0.3 K and 1.3 K, respectively, which indicates a fair distribution also. The symmetrical distributor was placed in a vertically downward direction in order to reduce the possibility of flow maldistribution in the evaporator. To check the uniformity of the refrigerant distribution, the surface temperature of each evaporator circuit was measured with thermocouples as

illustrated in Figure 10. The measured surface temperatures of the inlet and outlet of each evaporator circuit and the intermediate path of the condenser circuits for all three refrigerants were comparable within 0.5 K and 1.0 K, respectively, which indicates an acceptable distribution.

Table 5: Specifications of Heat Exchangers

Specification		Evaporator	Condenser
Dimension	W x H x D [cm]	213 x 57 x 8	99 x 70 x 8
	Frontal area [m ²]	1.22	0.69
Air flow	Air flow rate [m ³ /s]	3.3	1.6
	Frontal air velocity [m/s]	2.67	2.35
Fin	Shape	Wavy	Wavy
	Fin pitch [mm]	3.6	2.1
	Thickness [mm]	0.19	0.13
Tube	No. of row	3	3
	No. of tubes per each row	18	22
	Tube diameter [mm]	9.52	9.52
	No. of circuit	9	3 (R-404A, R-290), 2 (R-410A)
	Tube shape	Inner grooved	Inner grooved

Compressor

The test unit employs a scroll compressor from Copeland Corp. Three scroll compressors having different displacement volume as shown in Table 6 were used. All compressors were sized to produce as closely as possible the same cooling capacity for each respective refrigerant and use the motors having the closest possible motor efficiency. Since the selected largest displacement volume available for R-290 is still smaller than the target displacement, an inverter drive was used to match the refrigeration capacity by adjusting the inverter. Two different lubricants were utilized in testing, POE for R-404A and R-410A, and mineral oil for R-290. This requires system flushing in addition to compressor changes. After draining the oil used in the previous test, another compressor was installed and new oil charged and drained repeatedly until the index of refraction of the oil becomes that of the new oil to be used for the following test. Then the appropriate compressor, precharged with the correct lubricant, was installed.

Table 6: Specifications of Compressors

Refrigerant	R-404A	R-410A	R-290
Oil	POE	POE	Mineral oil
Displacement [cc]	77.2	54.2	82.6
Displacement Volume Ratio	1	0.70	1.07
Motor	3 phase, 208-230 V AC, 60 Hz		

Expansion Device

A single hand adjusted needle valve was used as the expansion device between the condenser and evaporator in the system in order to maintain an equal evaporator superheating for all three refrigerants.

Vapor Line

It should be noted that to minimize the effect of the pressure drop across the vapor suction line on the system performance, the pressure drop across the suction line was always maintained less than 1 K saturation temperature drop by using 15.8 mm tube diameter and 5 m length for the suction line. In applications with longer and smaller suction line, R-410A may have more benefit due to its lower pressure drop.

Receiver

A typical commercial refrigeration system has a receiver for refrigerant management. However, in this study the receiver was not utilized in the test unit to minimize the refrigerant charge for R-290 for safety reasons and to match simulation conditions.

Refrigerants

Two HFC's (R-404A and R-410A) were supplied from Honeywell and propane was purchased from a local chemical supplier. Since the refrigerant purity of two HFC's is higher than 99.5% (ARI Standard 700, 1999), the effects of impurities are negligible. There are three grades of propane potentially used as the refrigerant (Table 7). Among the three major impurities in Table 7 (isobutane, butane and ethane), R-600a has the highest composition and can potentially affect the property of propane. Since the boiling temperature of R-600a is higher than R-290, more R-600a means a higher saturation temperature. The saturated liquid temperatures of instrument grade and chemically-pure grade are very similar to that of pure R-290 within a 0.2 K deviation. The saturated vapor temperatures of these two grades are 0.2 – 0.3 K and 0.5 K higher than that of pure R-290, respectively. However, these differences are almost the same as the thermocouple measurement error. Moreover, the saturation enthalpies and densities of these three grades are almost the same within 0.1% variation. The difference in the refrigerant side capacity calculated by assuming pure R-290 and the other two grades is less than 0.5%. Therefore, three grades shown in Table 7 can be technically treated as pure R-290. In the R-290 testing, the instrument grade was used.

Table 7: Impurities of Propane (Airgas, 2003)

Grade	Composition [wt.%]			
	Propane (C ₃ H ₈)	Isobutane (C ₄ H ₁₀)	Butane (C ₄ H ₁₀)	Ethane (C ₂ H ₆)
Research grade	99.99	< 0.01	< 0.01	< 0.01
Instrument grade	99.53	0.40	0.07	0.01
Chemically pure grade	98.98	0.77	0.20	0.03

5.6 Test Procedure

Test conditions for full load and part load conditions are summarized in Table 8. First the refrigerant charge was optimized to maximize the system COP by running a series of tests at full load conditions (ambient temperature at 35°C). During the charge optimization tests, the degree of superheating was kept constant to be 5 K by adjusting the opening of the metering valve to simulate the control of a TXV. The optimum refrigerant charge was decided when the COP became the maximum. Then the part load test (ambient temperature at 18.3°C) was conducted at the optimum charge that was determined from the full load tests. For both tests, the evaporator inlet air was kept at 1.7°C dry-bulb temperature and dry condition. Air flow rates

through the evaporator and condenser were fixed at 3.3 m³/s and 1.6 m³/s, respectively. Moreover all test data was acquired after the system reached steady-state.

Table 8: Test Conditions

Test	Heat Exchanger	Inlet air dry-bulb/wet-bulb temperature [°C]	Air flow rate [m ³ /s]	Superheating [K]
Full load	Evaporator	1.7/-2.0	3.3	5
	Condenser	35.0/24.0	1.6	
Part load	Evaporator	1.7/-2.0	3.3	5
	Condenser	18.3/11.0	1.6	

5.7 Full Load Test Results

Frequency Adjustment and Effects of Inverter

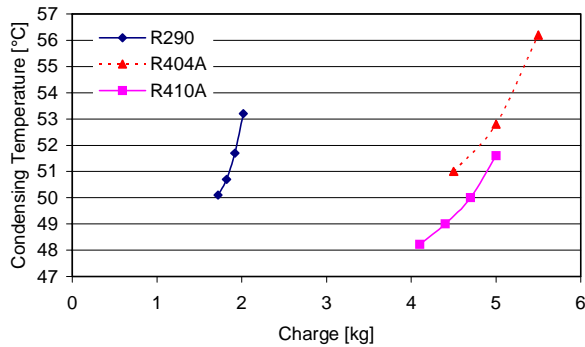
To compare the performance of each refrigerant under fair conditions, it was decided to match the cooling capacity of R-410A and R-290 to that of R-404A. Since the compressors were selected from the commercially available platform as shown in Table 6, the frequency of the inverter was varied in R-410A and R-290 testing. As a result of the frequency variation, 60 Hz and 66 Hz were selected for the inverter setting of R-410A and R-290, respectively. Moreover, R-410A was evaluated both using the inverter and without the inverter to investigate the effects of the inverter. Table 9 compares the performance and electrical characteristics of the two cases, with and without using the inverter. As shown in Table 9, by using the inverter the input line voltage dropped by 5 V but the current and power consumption of the compressor were only changed within 0.2% between two cases. Furthermore, the difference of the performance between with and without using the inverter is less than 1% in the performance. Similar results were found for R-290 as well.

Table 9 Effects of Using Inverter on Electrical Characteristics and Performance of R-410A

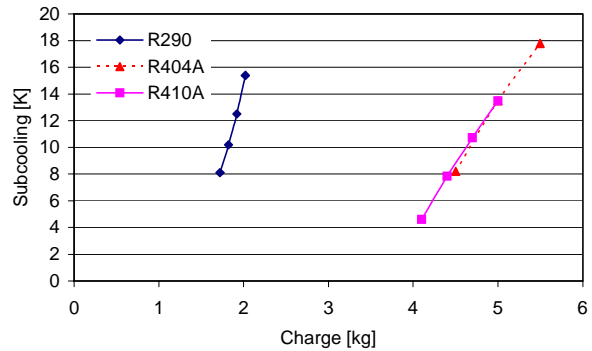
	Parameter	With inverter	Without inverter	Difference
Electrical characteristics	Frequency [Hz]	60	60	0
	Voltage [V]	208	213	+ 5
	Current [A]	15.7	15.7	0
	Compressor power [kW]	4.987	4.975	- 0.012
Performance	Charge [kg]	4.7	4.7	0
	Capacity [kW]	10.7	10.6	- 0.1
	COP	1.71	1.70	- 0.1
	DP_{evap} [kPa]	18.1	17.8	- 0.3
	DP_{cond} [kPa]	198	200	+ 2
	$P_{evap,avg}$ [kPa, abs]	694	687	- 7
	$P_{cond,avg}$ [kPa, abs]	3,073	3,075	+ 2
	Subcooling [K]	10.6	11.1	+ 0.5
	Superheating [K]	4.7	5.2	+ 0.5
	Pressure Ratio	4.63	4.68	+ 0.05
	Mass flow rate [g/s]	70	69	- 1
	η_{vol}	0.89	0.89	0
	η_{comp}	0.63	0.63	0

Charge Optimization

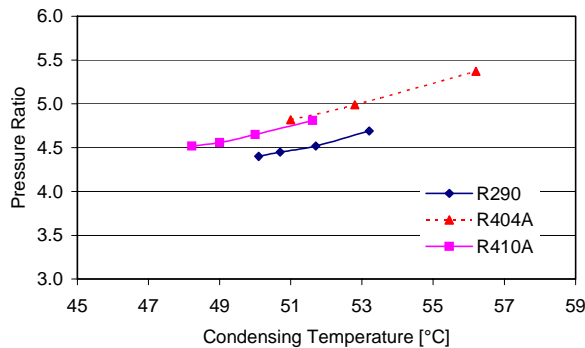
The charge optimization tests were performed under full load conditions. By varying the refrigerant charge, the optimum charge resulting in the highest COP was experimentally obtained. It should be noted that the power consumption of the unit cooler and condensing unit excluding that of the compressor was constant at 0.91 and 0.34 kW, respectively throughout all tests. As described earlier, the compressor line frequency was adjusted during the R-410A and R-290 charge optimizations to match the cooling capacity to that of R-404A within 1%. When the refrigerant charge was increased with the fixed degree of the superheating, the condensing temperature and the degree of subcooling increased as shown in Figure 11 (a) and (b). This increase of the subcooling contributed to the higher latent heat of evaporation. At the same time, the higher condensing temperature yielded a higher pressure ratio, which contributed to the higher compressor work as shown in Figure 11 (c) and (d).



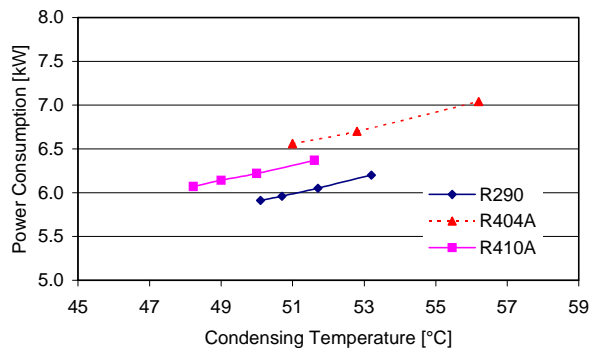
(a) Condensing Temperature vs. Charge



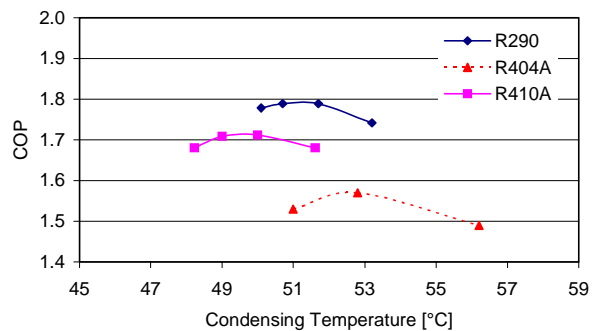
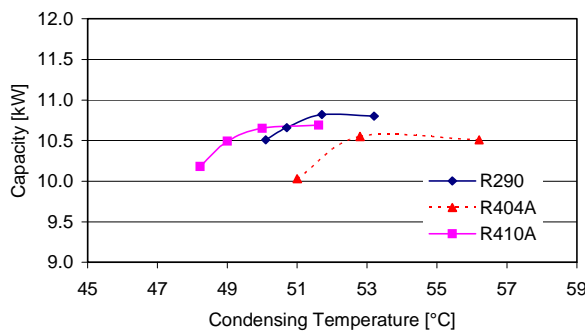
(b) Subcooling vs. Charge



(c) Pressure Ratio vs. Condensing Temp.



(d) Power Consumption vs. Condensing Temp.



(e) Capacity vs. Condensing Temp.

(f) COP vs. Condensing Temp.

Figure 11: Charge Optimization Results

However, the effective increase of the available latent heat of evaporation diminishes as the condensing temperature increases as can be seen from the pressure-enthalpy diagram of each refrigerant while the compressor work keeps increasing. Therefore, the refrigeration capacity and COP increase until they reach their maximum and then decrease as illustrated in Figure 11 (e) and (f). The system performance of the three refrigerants as well as their cycle parameters at three different charges is summarized in Table 10. The optimum charge of R-404A was 5.0 kg with a capacity of 10.6 kW and the COP was 1.57. The optimum charge of R-410A and R-290 was 94% and 36% of that of R-404A. The COPs of R-410A and R-290 were 9% and 14% higher than those of R-404A. This result reflects the thermodynamic characteristics of R-410A and R-290.

The performance of all three refrigerants calculated for two ideal cycle conditions are compared in Table 11. In this calculation, the following conditions were assumed for an ideal cycle: zero subcooling, zero pressure drop across the heat exchangers, 100% compressor efficiency. It shows a 6% and 12% higher COP as compared to R-404A for R-410A and R-290 respectively under the first condition in Table 11, which is a typical compressor test condition. It also shows a 9% and 14% higher COP for R-410A and R-290, respectively under the second condition in Table 11, which has a reduced degree of superheating and is close to the system test condition. Table 11 also indicates that the pressure ratio (PR) of R-410A is 1% higher than that of R-404A but the PR of R-290 is 5% lower, which results in a thermodynamically more favorable compressor operating condition for R-290. Even though this comparison explains the inherent thermodynamic difference, further analysis, which can account for the effects of the heat transfer, pressure drop, and subcooling is required because the actual system operating conditions are different from the ideal conditions used in this comparison.

Table 10: Full Load Test Results (Optimum charge in bold)

Refrigerant	Parameter	Data		
R-404A (60 Hz)	Charge [kg]	4.5	5.0	5.5
	Capacity [kW]	10.0	10.6	10.5
	COP	1.53	1.57	1.49
	DP_{evap} [kPa]	29.8	29.4	28.7
	DP_{cond} [kPa]	136	130	120
	$P_{evap,avg}$ [kPa, abs]	529	530	529
	$P_{cond,avg}$ [kPa, abs]	2,354	2,450	2,649
	Subcooling [K]	8.2	13.5	17.8
	Superheating [K]	5.5	5.3	5.4
	Pressure Ratio (P_{dis}/P_{suc})	4.82	4.99	5.37
	T_{evap}/T_{cond} at P_{suc}/P_{dis} [°C]	-5.4/52.4	-5.4/54.0	-5.4/57.4
	Mass flow rate [g/s]	100	100	99
	η_{vol}	0.91	0.91	0.91
	η_{comp}	0.61	0.600	0.59
	R-410A (60 Hz)	Charge [kg]	4.4	4.7
Capacity [kW]		10.5	10.7	10.7
COP		1.71	1.71	1.68
DP_{evap} [kPa]		18.0	17.8	17.7
DP_{cond} [kPa]		222.9	202	186
$P_{evap,avg}$ [kPa, abs]		691	690	690
$P_{cond,avg}$ [kPa, abs]		2,995	3,064	3,179
Subcooling [K]		7.8	10.7	13.5
Superheating [K]		5.2	5.0	4.9
Pressure Ratio (P_{dis}/P_{suc})		4.56	4.65	4.81
T_{evap}/T_{cond} at P_{suc}/P_{dis} [°C]		-5.4/51.4	-5.4/51.9	-5.2/52.8
Mass flow rate [g/s]		70	70	69
η_{vol}		0.90	0.89	0.89
η_{comp}		0.64	0.635	0.63
R-290 (66 Hz)		Charge [kg]	1.7	1.8
	Capacity [kW]	10.5	10.7	11.1
	COP	1.78	1.79	1.79
	DP_{evap} [kPa]	17.0	16.5	16.4
	DP_{cond} [kPa]	98	92	84
	$P_{evap,avg}$ [kPa, abs]	416	416	418
	$P_{cond,avg}$ [kPa, abs]	1,716	1,741	1,778
	Subcooling [K]	8.1	10.2	12.5
	Superheating [K]	5.5	5.7	5.2
	Pressure Ratio (P_{dis}/P_{suc})	4.40	4.45	4.52
	T_{evap}/T_{cond} at P_{suc}/P_{dis} [°C]	-4.9/50.6	-5.0/51.4	-5.2/52.8
	Mass flow rate [g/s]	42	42	42
	η_{vol}	0.94	0.93	0.93
	η_{comp}	0.65	0.647	0.64

Table 11: Thermodynamic Comparison of Three Refrigerants

Condition	Refrigerant	COP Ratio	PR Ratio
-6.7/48.9/7.2/0 ($T_{evap}/T_{cond}/T_{suc}/\text{Subcool}$)	R-410A/R-404A	1.06	1.01
	R-290/R-404A	1.12	0.95
-6.7/48.9/-1.1/0 ($T_{evap}/T_{cond}/T_{suc}/\text{Subcool}$)	R-410A/R-404A	1.09	1.01
	R-290/R-404A	1.14	0.95

(zero subcooling, zero pressure drop across the heat exchangers, 100% compressor efficiency)

Condensation Heat Transfer

Since the same air-side conditions were used for all refrigerants with equal capacity, the refrigerant-side thermal resistance is responsible for the difference in overall condenser thermal resistance and pressure drop, and thus for the pressure ratio of each refrigerant. Table 12 compares the ratio of the measured refrigerant mass flux and average condensation heat transfer of R-410A and R-290 as compared to those of R-404A utilizing Cavallini's condensation heat transfer correlation (1999). If it is assumed that the refrigerant-side thermal resistance reduction by enhancing the refrigerant-side heat transfer contributes to approximately one third of the overall thermal resistance reduction at the given amount of the condenser heat, then the condensing temperature of R-410A and R-290 could be reduced by 2.8 K and 0.6 K as compared to that of R-404A. This result indicates R-410A has a better condensation heat transfer than R-290, which is different from the earlier conclusion of the transport property analysis. This occurs due to the changes in the refrigerant mass flux, the mass flux increase of R-410A by reducing the number of parallel circuits and the mass flux decrease of R-290, which is another dominant heat transfer factor. This qualitative reasoning would help in understating the effects of the condensation heat transfer enhancement on the condensing temperature decrease of R-410A and so does the pressure ratio. However, the actual condensing temperature of R-290 is similar to that of R-410A. This is due to the reduced pressure drop of R-290 due to the smaller mass flux, which is only half of that of R-410A, and the enhanced compressor efficiency as further discussed below.

Table 12: Contribution of Condensation Heat Transfer

Refrigerant	Mass flux ratio	Average condensation heat transfer ratio	Condensing temperature decrease [K]
R-410A/R-404A	1.05	1.56	2.8
R-290/R-404A	0.42	1.11	0.6

It should be noted that the effect of the receiver can be different for each refrigerant. The condensing temperature would be lower than that for the current test results when a receiver is used for R-404A and R-410A. The use of the receiver was not feasible for R-290 for safety reasons.

Compressor Efficiency

Figure 12 illustrates the measured compressor efficiency of the three refrigerants as defined by equation (7). As shown here, the compressor efficiency varies as a function of the pressure ratio. Since a higher compressor efficiency would mean a smaller compressor power consumption, the lower pressure ratio is desirable and can be achieved with better heat exchanger design.

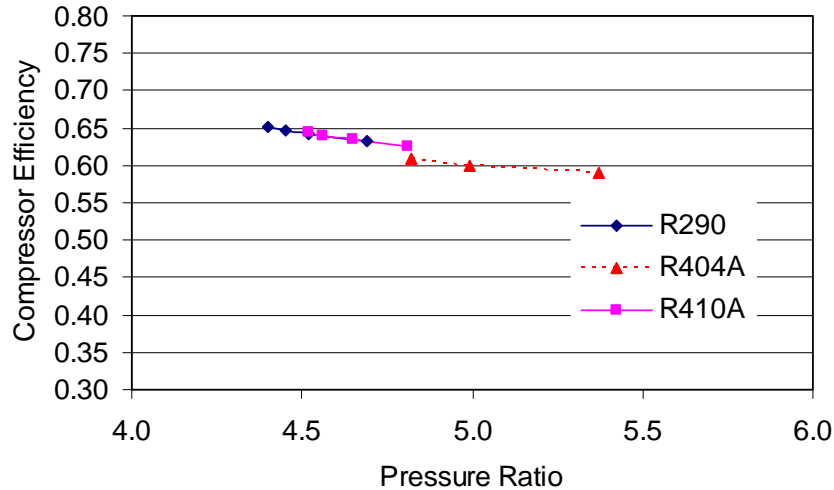


Figure 12: Compressor Efficiency vs. Pressure Ratio

As can be seen from Table 11, the theoretical pressure ratio of R-290 is 5% lower than that of R-404A, improving the compressor efficiency by approximately 3%. Whereas, the measured pressure ratio of R-290 is 11% lower than that of R-404A, which is attributed to the better condensation heat transfer in addition to the relatively lower vapor pressure at elevated temperatures. However, it should be noted that the compressor efficiency is also affected by the compressor design in addition to the above two factors.

Effects of Compressor Efficiency under Full-Load Conditions

Production compressors were selected to match the capacity requirement of each refrigerant as closely as possible. Since the compressor is optimized based on a pre-determined built-in scroll set volume ratio, it may not be as optimized under a higher or lower pressure ratio that may occur under the system operating condition. According to the compressor manufacturer, the same compressor efficiency can be expected, if each compressor is optimized for each refrigerant at the system operating condition by adjusting the built-in scroll set volume ratio and the motor. Table 13 compares the system performance of the three refrigerants for two cases. The first case is based on the measured compressor efficiency from Table 10. The second case is based on the recalculation of the compressor power assuming the compressor efficiency of R-410A and R-290 being equal to that of R-404A. This adjustment is intended to compare the performance of each refrigerant while eliminating the effect of the compressor efficiency assuming the compressor manufacturer could achieve the same compressor efficiency for each refrigerant. Then the COP improvement of R-410A and R-290 over R-404A is reduced to 4% and 7%, respectively.

Table 13: Effects of Compressor Efficiency under Full Load Conditions

Case	Refrigerant	Compressor Efficiency Ratio	COP Ratio
Based on measured value (from Table 10)	R-410A/R-404A	1.06	1.08
	R-290/R-404A	1.08	1.14
Assuming equal compressor efficiency	R-410A/R-404A	1.00	1.04
	R-290/R-404A	1.00	1.07

5.8 Part Load Test Results

After finishing all full load tests, the part load tests (ambient temperature at 18.3°C) were conducted at the optimum charge that was determined from the full load tests. Table 14 shows the comparison of part load test results. The capacity of R-290 was 2% lower than that of R-404A but the capacity of R-410A was the same. The measured COPs of R-410A and R-290 were 10% and 11% higher than the one of R-404A. This result illustrates that the COP of R-410A over R-404A is further enhanced by 2% but the performance of R-290 over R-404A is reduced by 3% when the operating conditions change from the full load to part load. As a result, the performance enhancement of the R-410A is essentially the same as that of R-290 under part load conditions. These changes in the performance with the load condition agree well with the theoretical cycle efficiency comparison as illustrated in Figure 3.

Table 14: Part Load Test Results

Refrigerant	R-404A	R-410A	R-290
Frequency [Hz]	60	60	66
Charge [kg]	5.0	4.7	1.8
Capacity [kW]	12.9	12.9	12.5
COP	2.39	2.64	2.66
DP_{evap} [kPa]	28.7	18.4	16.8
DP_{cond} [kPa]	135	282	108
$P_{evap,avg}$ [kPa, abs]	510	674	405
$P_{cond,avg}$ [kPa, abs]	1,675	2,050	1,185
Subcooling [K]	12.0	7.7	6.1
Superheating [K]	5.8	5.2	5.9
Pressure Ratio (P_{dis}/P_{suc})	3.61	3.30	3.18
Mass flow rate [g/s]	100	72	43
η_{vol}	0.94	0.93	0.97
η_{comp}	0.66	0.69	0.70

Effects of Compressor Efficiency under Part Load Conditions

Similar to the full load condition, Table 15 compares the system performance of the three refrigerants for two cases. The first case is based on the measured compressor efficiency from Table 14. The second case is based on the recalculation of the compressor power consumption assuming the compressor efficiency of R-410A and R-290 being equal to that of R-404A. Then the COP improvement of both R-410A and R-290 is reduced to 7%.

Table 15: Effects of Compressor Efficiency under Part Load Conditions

Case	Refrigerant	Compressor Efficiency Ratio	COP Ratio
Based on measured value (from Table 14)	R-410A/R-404A	1.04	1.10
	R-290/R-404A	1.06	1.11
Assuming equal compressor efficiency	R-410A/R-404A	1.00	1.07
	R-290/R-404A	1.00	1.07

5.9 Comparison of Simulation and Experimental Results

To verify the Genesym model used in the condenser design, results from the model and test were compared for the cycle parameters as shown in Table 16. The modeled evaporating

temperatures match the test results within 0.8 K, while the modeled condensing temperatures are 2 K to 4 K lower than the test results, which are larger deviations than those for the evaporating temperatures. Degrees of subcooling and superheating match the test results within 0.6 K. Compressor efficiencies predicted by the compressor map based model show values 0.2% to 2.1% higher than the test results.

Table 16: Comparison of Cycle Parameters between Model and Test Results

Difference between model and test results	Evaporating temperature [K]	Condensing temperature [K]	Degree of Subcooling [K]	Degree of superheating [K]	Compressor efficiency [%]
R-404A	-0.5	-2.2	0.5	-0.5	2.1
R-410A	0.8	-3.8	0.4	-0.1	0.2
R-290	0.2	-3.4	0.1	-0.6	0.7

(Base: test results)

A second simulation was conducted using “Coil Designer” and “Vapcyc” of CEEE. A comparison of the two simulations and the test results of the charge optimization for each refrigerant was conducted as illustrated in Figure 13. Generally the simulation with Genesym shows a slightly higher efficiency at somewhat lower subcooling (or refrigerant charge) while the simulation with CEEE model (Coil Designer and Vapcyc) shows a slightly lower efficiency at similar subcooling. The differences between models and experimental data are within $\pm 5\%$, which is within the expected accuracy of the simulation and testing. Genesym consistently over predicts the COP within 5% and the CEEE model consistently under predicts the COP within 5%. Furthermore, all deviations are of the same order of magnitude and in the same direction for all refrigerants.

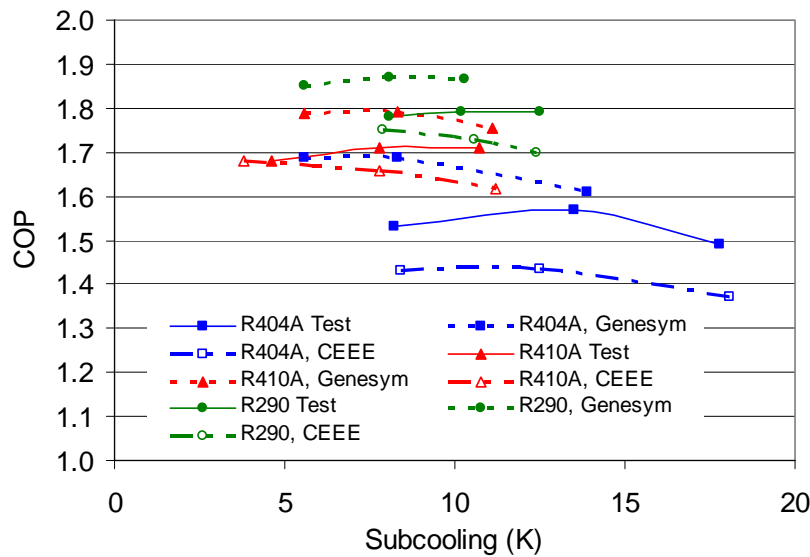


Figure 13: Comparison of Simulation and Experimental Results

6 LIFE CYCLE CLIMATE PERFORMANCE (LCCP) ANALYSIS

There are two types of global warming effect. The first one is the direct global warming contribution due to the emission of refrigerants itself. The second is the indirect global warming contribution due to the emission of CO₂ by consuming the energy which is obtained by combustion of fossil fuels. In order to determine the effect of the refrigerants investigated and to analyze both the direct and indirect contributions to global warming calculations were conducted by applying the similar approach used by Spatz and Motta (2003).

6.1 Safety Issue and Energy Efficiency

To meet the safety requirement for R-290 system, the first cost of R-290 systems would increase up to 30% as estimated by Threadwell (1994) for a typical residential unit. Powell et al. (2000) also reported the cost increase of HC's related with the electrical safety enhancement as much as \$240 to \$500 for commercial refrigeration and air-conditioning type applications. If a moderate cost increase of 10% of the first cost is used to enhance the efficiency of HFC blends, this will result in a lower LCCP for HFC blends. To investigate this scenario, it was assumed that a 10% increase in the first cost was used to increase the condenser height and tube length by 20% and 23%, respectively resulting in a 48% increased face area. Furthermore, it was assumed that a bigger fan was used to maintain the same air velocity. The resulting increase in the fan power consumption was accounted for in the calculation. Then the system simulation result of using a larger condenser shows how the condensing temperature decreases compared to the condenser tested as shown in Table 17. In Table 17, the condensing temperature is calculated from the saturated vapor temperature at the compressor discharge pressure. As can be seen from Table 17, the condensing temperature of R-404A is approximately 2 K to 3 K higher than that of R-290 with a condenser tested but reaches in the same level when a larger condenser is used for both. According to the system manufacturer, the condensing temperature level, 51.4°C to 54.0°C, for the system with the condenser tested is rather higher than that of representative typical design practice. Moreover, the simulation of the system with a 48% larger condenser resulted in condensing temperatures of 46.0°C to 47.6°C, which are representative of typical design practice. Therefore, it can be said that the condenser tested is smaller than the typical condenser size. Since the larger condenser yields customary condensing temperatures used in typical commercial condenser design, it is referred to as "typical condenser" hereafter. Whereas the condenser tested is referred to as "small condenser" hereafter. The decrease in the condensing temperature would result in a system COP enhancement by improving the compressor efficiency. Table 18 summarizes the compressor efficiency for both condenser cases. Here, the compressor efficiency for the small condenser case is based on the measured data from the current study and the change in compressor efficiency for the typical condenser is based on the compressor performance map based model.

Table 17: Effects of Condenser on Condensing Temperature

Refrigerant	R-404A	R-410A	R-290	R-404A	R-410A	R-290
Load condition	Part	Part	Part	Full	Full	Full
Condensing temp. of small condenser [°C]	38.3	36.0	35.7	54.0	51.4	51.9
Condensing temp. of typical condenser [°C]	31.4	29.8	31.5	47.6	46	47.5
Condensing temp. change [K]	6.9	6.2	4.2	6.4	5.4	4.4

Table 18: Effects of Condenser on Compressor Efficiency under Full Load Conditions

Refrigerant	Compressor efficiency for small condenser (from test data) [%]	Compressor efficiency for typical condenser (from model) [%]
R-404A	60.0	64.4
R-410A	63.5	64.8
R-290	64.7	65.6

Since the model results show a similar compressor efficiency when the typical condensing temperature is used for the three refrigerants, further comparisons were conducted in three scenarios based on an equal compressor efficiency basis as illustrated in Figure 14. The first scenario implies that the test data are reevaluated on the equal compressor efficiency based on the measured R-404A value. Then the COP differences between two HFC blends and R-290 are reduced by 5% to 2% (at full load condition) and 4% to 1% (at part load condition) for R-404A and R-410A, respectively as compared to the measured data. The second scenario implies that a typical condenser is used for all three refrigerants and that the compressor efficiency is the same for all. The simulation results for R-404A and R-410A with a typical condenser show 10% to 14% (at full load condition) and 7% to 9% (at part load condition) COP enhancement respectively over R-290 as compared to the test data with a small condenser. Moreover, the COP enhancement of both HFC blends by using a typical condenser is larger under part load conditions than under full load conditions. The third scenario implies that the unit first cost is matched for the three refrigerants by assuming that a typical condenser is used for only HFC blends and additional safety features are used only for R-290. Again, the underlying assumption is that the first cost of the R-290 system may be, for example, 10% higher due to added safety features, and on an equal cost basis, the HFC systems would use the additional cost for a larger condenser. In this case, the condensing temperatures of HFC blends are 4 K to 6 K lower than that of R-290. Moreover, the COP of R-404A is comparable to that of R-290 within 4% and the COP of R-410A is 2% to 8% higher than that of R-290. Since the COP enhancement directly affects the results of LCCP analysis, it was decided to include the typical condenser case in the LCCP analysis.

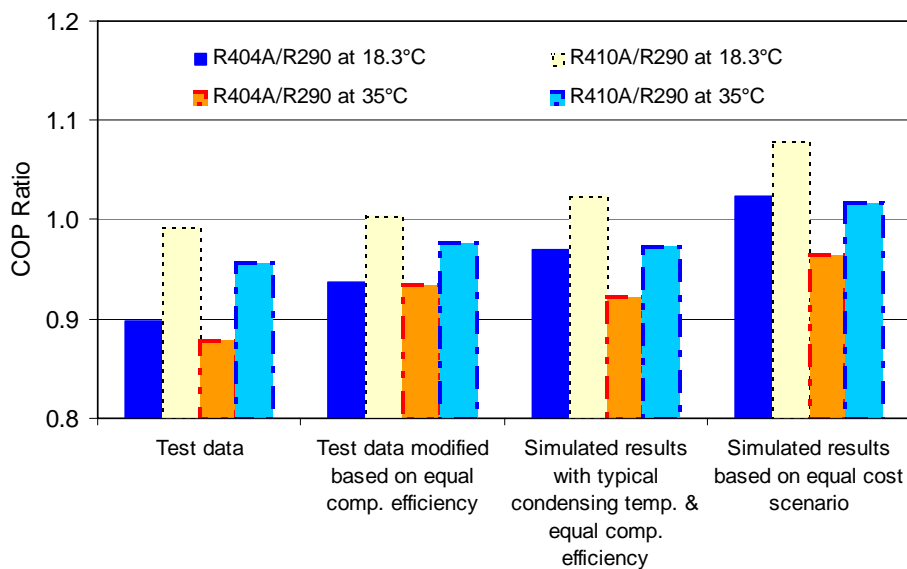


Figure 14: Comparison of COP

6.2 LCCP Comparison

The environmental impact of refrigerants over the entire lifecycle of fluid and equipment, including power consumption, is captured in the life cycle climate performance (LCCP) value. The lower the value, the lower the environmental impact. In order to determine the power consumption of a typical refrigeration system over the course of a year, a bin analysis was performed using weather data from an ARI Standard for chillers (ARI Standard 550, 1998). It uses data averaged from 29 cities across the U.S. Table 19 shows the results of this analysis which was used to determine the indirect global warming contribution by extrapolating the test results under the full load and part load conditions. Four assumptions used in the ADL report (2002) were used: a 0.65 kg of CO₂ per kW-hr of electrical production, a 2% annual leakage rate, a 15% end-of-life loss, and a 15-year life. It should be noted that these assumptions were taken from a split unitary a/c system since test equipment consisting of the condensing unit and unit cooler for the walk-in cooler application is very similar in design.

Table 19: System Power Consumption - Weather Bin Analysis

Temp. bin (°C)	Hrs	Load Ratio	kW-hours					
			With small condenser			With typical condenser		
			R-404A	R-410A	R-290	R-404A	R-410A	R-290
36.4	37	1.000	255	236	223	245	230	220
33.6	120	0.975	746	686	656	705	665	644
30.8	303	0.950	1,705	1,565	1,511	1,592	1,507	1,478
28.1	517	0.925	2,648	2,425	2,360	2,447	2,320	2,299
25.3	780	0.900	3,652	3,336	3,271	3,342	3,175	3,175
22.5	929	0.875	3,988	3,636	3,588	3,620	3,444	3,471
19.7	894	0.850	3,529	3,212	3,187	3,179	3,029	3,074
16.9	856	0.825	3,114	2,831	2,822	2,787	2,658	2,714
14.2	777	0.800	2,611	2,369	2,373	2,322	2,216	2,276
11.4	678	0.775	2,107	1,910	1,920	1,863	1,780	1,837
8.6	2,869	0.750	8,255	7,475	7,544	7,262	6,946	7,200
Total	8,760	-	32,610	29,682	29,455	29,364	27,971	28,387

With this information, a life cycle climate performance (LCCP) analysis was performed for five cases and results are shown in Figure 15. The LCCP analysis shows that R-404A and R-410A have 13% and 1% higher LCCP, respectively than that of R-290 when the small condenser is used for all three refrigerants. However, when the LCCP is recalculated for HFC blends having a typical condenser, the LCCP of R-404A and R-410A decreases by 10% and 5%, respectively, as compared to the small condenser case. The LCCP of R-404A is 6.5% higher than that of R-290 and the LCCP of R-410A is equal to that of R-290 when a typical condenser, which yields condensing temperatures of 46.0°C to 47.6°C, is used for all three refrigerants. The LCCP of R-404A and R-410A with a typical condenser is 1.8% higher and 4.2% lower, respectively than that of R-290 with a small condenser as shown in Figure 15. Furthermore, it is very clear from these results that the indirect contributions dominate any contributions from refrigerant emissions.

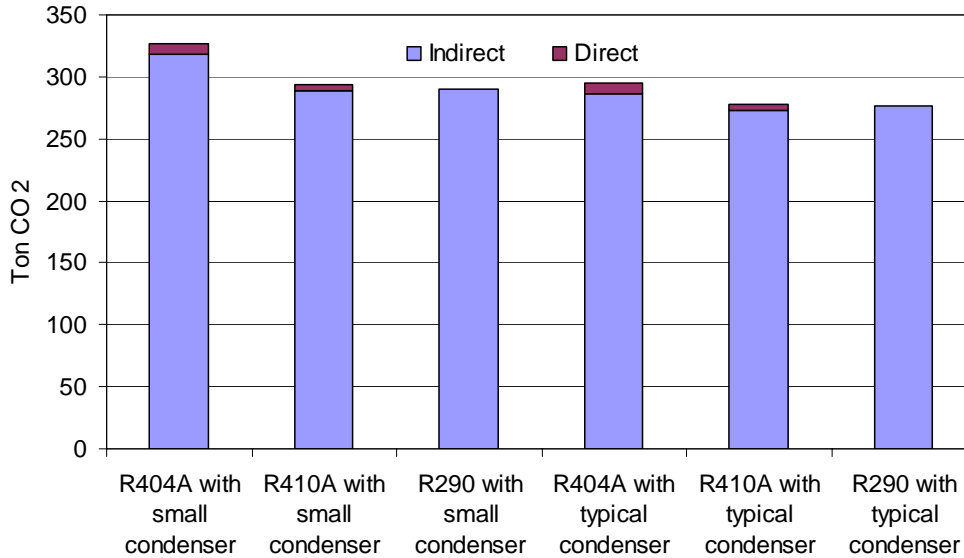


Figure 15: Comparison of LCCP

7 CONCLUSIONS

Due to growing environmental awareness and resulting concerns, refrigerants, the working fluids for refrigeration systems, heat pumps and air conditioners, have attracted considerable attention. Policies to reduce global warming force industry to develop technologies that can reduce emissions and improve energy efficiency. Despite the flammability of hydrocarbons, some refrigerator manufacturers especially in European countries and Japan have started employing hydrocarbons as refrigerants predominantly in small capacity equipment. These issues have led to calls for the careful investigation of currently used refrigerants (HFC's) and potentially applicable HC refrigerants (R-290). To help provide a clearer understanding of the relative performance potential of the R-290 as compared to two HFC's (R-404A and R-410A) for medium temperature commercial refrigeration, CEEE started an experimental evaluation program under ARI's GREEN Program.

A new experimental facility to test the performance of three refrigerants for medium temperature commercial refrigeration was designed and fabricated for this study. A 11 kW refrigeration system consisting of a unit cooler and a condensing unit, which was originally designed for R-404A, served as the test unit. To match the capacity between refrigerants, compressors having a 30% smaller and 7% larger displacement volume than for R-404A were selected for R-410A and R-290. Since the displacement volume of the R-290 compressor was slightly smaller than the target displacement, a higher frequency of 66 Hz was used to match the refrigeration capacity by using an inverter drive. For safety reasons it was decided to minimize the charge of the R-290 test unit by eliminating the refrigerant receiver. The condenser was also modified to contain a liquid sub cooler circuit. In order to maintain a consistent comparison, the receiver was also eliminated from the test units for R-410A and R-404A as well as all equipment modeled in simulations. Based on the optimization of the condenser, which is the most critical component of the medium temperature commercial refrigeration system, a two circuit condenser was used for the testing of R-410A while a three circuit condenser was used for the testing of R-404A and R-290. The air side of all condensers was identical. By operating these systems in the

newly constructed test facility, full load and part load tests were conducted under only sensible heat transfer conditions.

Charge optimization tests of three refrigerants were completed at the full load condition. Result shows that the optimum charge of R-404A was 5.0 kg while the optimum charge of R-410A and R-290 was 94% and 36% of R-404A charge. Once the refrigerant charge was optimized, each refrigerant was tested both under full load and part load conditions. Based on equal system capacity tests, the COPs of R-410A and R-290 were 9% and 14% higher than that of R-404A under the full load condition, and they were 10% and 11% higher under the part load condition. This result illustrates that the performance enhancement of R-290 as compared to R-404A is 5% better than that of R-410A under full load conditions at about 51.4°C to 54.0°C condensing temperatures. Moreover, the performance enhancement of R-410A is approximately the same as that of R-290 under part load conditions. The enhancement of R-410A over R-404A stems from the better condensation heat transfer, which reduces the condensing temperature and the pressure ratio. The enhancement of R-290 over R-404A stems from both an inherent thermodynamic property of R-290 (lower pressure ratio) and better condensation heat transfer, which reduces the condensing temperature and the pressure ratio. If it is assumed that the same compressor efficiency could be achieved by optimizing the compressor for each refrigerant, then the COP improvement of both R-410A and R-290 over the current experimental data is reduced to 4% with R-410A and to 7% with R-290 under full load conditions, and to 7% for both R-410A and R-290 under part load conditions.

In order to determine the environmental impact of the refrigerants investigated, an LCCP analysis was conducted. According to the system manufacturer, the measured condensing temperature level, 51.4°C to 54.0°C, is higher than that of representative typical design practice. The simulation of the system with a condenser having a 48% larger surface area resulted in condensing temperatures of 46.0°C to 47.6°C, which are representative of typical design practice. Therefore, both systems were investigated in the LCCP analysis with the condenser as tested (referred to as “small condenser”) and with a 48% larger condenser (referred to as “typical condenser”).

To fairly compare the LCCP, it is assumed that the same cost increase of 10%, for R-290 to meet safety requirements, is equivalent to the cost of the 48% extra condenser surface area used to enhance the efficiency of the two HFC blends. The system simulation results of using a typical condenser for R-404A and R-410A show a 10% to 14% and 7% to 9% COP enhancement, respectively as compared to the small condenser case. In the previous stated percentage range, the first value refers to the full load test and the second refers to the part load test.

The LCCP analysis shows that when a small condenser is used for all three refrigerants, R-404A and R-410A have 13% and 1% higher LCCP, respectively than that of R-290. However, when the LCCP is recalculated for all three refrigerants in systems with a typical condenser, the LCCP of R-404A is 6.5% higher than that of R-290 and the LCCP of R-410A is equal to that of R-290. On an equal first cost basis assuming the cost increase of 10% for R-290 to meet the safety requirements, matches the cost of the larger condenser for R-404A and R-410A, the LCCP of R-404A and R-410A is 1.8% higher and 4.2% lower, respectively, than that of R-290. Furthermore, it is very clear from these results that the indirect contributions dominate any contributions from refrigerant emissions.

Working fluid selection should consider many aspects including safety (toxicity and flammability), environmental impact (stratospheric ozone and climate change), cost and

performance (capacity and COP). The two most representative commercial refrigeration configurations are the direct expansion and distributed systems, either of which could potentially release the refrigerant into human occupied space. Therefore, the use of either flammable or high toxicity refrigerants is not feasible. To limit these cases, potentially hazardous refrigerants are limited to unoccupied spaces. In practice, condensing units with hydrocarbon refrigerants would be used in secondary loop systems. The secondary loop system may require additional cost and energy penalties due to the additional heat exchanger and pumping requirements and the use of heat transfer fluids. Therefore, a comparison of the secondary loop R-290 system to direct HFC cooling systems should be conducted.

8 REFERENCES

1. Arthur D. Little (ADL), 2002, Global Comparative Analysis of HFC and Alternative Technology for Refrigeration, Air Conditioning, Foam, Solvent, Aerosol Propellant, and Fire Protection Applications.
2. Air-Conditioning and Refrigeration Institute, 1989, Unitary Air-Conditioning and Air Source Heat Pump Equipment, *ARI Standard 210/240*.
3. Air-Conditioning and Refrigeration Institute, 1999, Standard for Unit Coolers for Refrigeration, ANSI/ARI Standard 420.
4. Air-Conditioning and Refrigeration Institute, 1997, Standard for Positive Displacement Condensing Units, ANSI/ARI Standard 520.
5. Air-Conditioning and Refrigeration Institute, 1997, Positive Displacement Refrigerant Compressors and Compressor Units, ANSI/ARI Standard 540.
6. Air-Conditioning and Refrigeration Institute, 1998, Standard for Water Chilling Packages Using the Vapor Compression Cycle, ANSI/ARI Standard 550.
7. Air-Conditioning and Refrigeration Institute, 1999, Standard for Specification for Fluorocarbon Refrigerants, ANSI/ARI Standard 700.
8. Airgas, 2003, Engineering Data.
9. American Society of Heating, Refrigerating, and Air-Conditioning Engineers, Inc., 2001, Fundamentals, *ASHRAE Handbook*.
10. American Society of Heating, Refrigerating, and Air-Conditioning Engineers, Inc., 2000, HVAC Systems and Equipment, *ASHRAE Handbook*.
11. American Society of Heating, Refrigerating, and Air-Conditioning Engineers, Inc., 1988, Method of Testing for Rating Unitary Air-conditioning and Heat Pump Equipment, *ASHRAE ANSI/ASHRAE 37*.
12. American Society of Heating, Refrigerating, and Air-Conditioning Engineers, Inc., 1980, Method of Testing for Rating Heat Operated Unitary Air-conditioning Equipment for Cooling, *ASHRAE ANSI/ASHRAE 40*.
13. American Society of Heating, Refrigerating, and Air-Conditioning Engineers, Inc., 1995, Methods of Testing for Seasonal Efficiency of Unitary Air-conditioners and Heat Pumps, *ASHRAE ANSI/ASHRAE 116*.
14. Beckwith, T., R. Marangoni, and J. Lienhard, 1993, Mechanical Measurements, Addison-Wesley Publishing Company.
15. Bivens, D.B., Yokozeki, A., Geller, V.Z., and Paulaitis, M.E., 1993, Transport properties and heat transfer of alternatives for R-502 and R-22, ASHRAE/NIST Refrigerants Conference, pp.73-84.

16. Cavallini, A., D. Col, D. Doretto, L. Longo, and L. Rossetto, 1999, Enhanced In-Tube Heat Transfer with Refrigerants, 20th International Congress of Refrigeration.
17. Chin, L. and Spatz, M.W., 1999, Issues relating to the adoption of R-410A in air conditioning systems, 20th International Congress of Refrigeration, IIR/IIF, Sydney.
18. IIR, 1997, Fluorocarbons and Global Warming, 12th Informatory Note of the IIR on Fluorocarbons and Refrigeration, International Institute of Refrigeration.
19. Choi, J.Y., Kedzierski, M.A., and Domanski, P.A., 1999, A Generalized Pressure Drop Correlation for Evaporation and Condensation of Alternative Refrigerants in Smooth and Micro-fin Tubes, NISTIR 6333.
20. Domanski, P.A., 1989, EVSIM – An Evaporator Simulation Model Accounting for Refrigerant and One-Dimensional Air Distribution, NIST Report, NISTIR 89-4133.
21. IPCC, 2001, Climate Change 2001- The Scientific Basis, Intergovernmental Panel on Climate Change, Cambridge University Press.
22. JARN, 2002, New Archives, 2002-Q3, www.jarn.co.jp.
23. Granryd, E., 1999, Hydrocarbons as Refrigerants-An Overview, *Proceedings of 20th International Congress of Refrigeration*, IIF/IIR, Sidney, Paper No. 732.
24. Greenpeace, 1997, *Greenpeace Website*, www.greenpeace.org/~ozone/.
25. Kline, S. and F. McClintock, 1953, Describing Uncertainties in Single-Sample Experiments, *Mech. Eng.*, Vol. 75, pp. 3-8.
26. NIST, 2002, REFPROP V7.0, *Reference Fluid Thermodynamic and Transport Properties*.
27. Treadwell, D.W., 1994, Application of R-290 to a Single Packaged Unitary Air-conditioning Product, ARI Flammability Workshop, ARI.
28. Powell, L., P. Blacklock, C. Smith, and D. Colbourne, 2000, The Use of Hydrocarbon Refrigerants in Relation to Draft U.K. Government Policy on Climate Change, *Proceedings of 4th IIR-Gustav Lorentzen Conference on Natural Fluids at Purdue*, pp.386-394.
29. Spatz, Mark and S. Motta, 2003, An Evaluation of Options for Replacing HCFC-22 in Commercial Refrigeration Systems, International Congress of Refrigeration, Washington, D.C., ICR0510.
31. UNEP, 2002, Report of the Refrigeration, Air-conditioning and Heat Pumps Technical Options Committee (RTOC) 2002 Assessment.
32. Wang, C.C., Jang, J.Y., and Chiou, N.F., 1999a. “A heat transfer and friction correlation for wavy fin-and-tube heat exchangers”, *International Journal of Heat Mass Transfer* 42, pp. 1919-1924.
33. Wang, C.C., Lee, C.J., Chang, C.T., and Lin, S.P., 1999b. “Heat transfer and friction correlation for compact louvered fin-and-tube heat exchangers”, *International Journal of Heat Mass Transfer* 42, pp. 1945-1956.
34. Wang, C.C., Chi, K.Y., and Chang, C.J., 2000, “Heat transfer and friction characteristics of plain fin-and-tube heat exchangers”, part II: correlation, *International Journal of Heat Mass Transfer* 43, pp. 2693-2700.
35. Wang, C.C., Lee, W.S., and Sheu, W.J., 2001. “A comparative study of compact enhanced fin-and-tube heat exchangers”, *International Journal of Heat Mass Transfer* 44, pp. 3565-3573.